Exogenous Smad3 Accelerates Wound Healing in a Rabbit Dermal Ulcer Model

Koji Sumiyoshi,*† Atsuhito Nakao,*§ Yasuhiro Setoguchi,‡ Ko Okumura,* and Hideoki Ogawa*†

*Atopy (Allergy) Research Center, Juntendo University School of Medicine, Tokyo, Japan; †Department of Dermatology, Juntendo University School of Medicine, Tokyo, Japan; ‡Department of Respiratory Medicine, Juntendo University School of Medicine, Tokyo, Japan; §Department of Immunology, Faculty of Medicine, University of Yamanashi, Yamanashi, Japan

Exogenous administration of transforming growth factor-β (TGF-β) improves wound healing by affecting cellular and molecular events involved in tissue repair. But mice with a deficiency of a key TGF-β signaling intermediate, Smad3, paradoxically showed accelerated cutanenous wound healing, suggesting that endogenous Smad3 had inhibitory effect on cutaneous wound healing. Here we investigated the effect of exogenous expression of Smad3 in dermal fibroblasts on cutaneous wound healing. Subcutaneous injection of adenovirus-containing Smad3 complementary DNA (AdCMV-Smad3) targeting mainly dermal fibroblasts accelerated tissue repair following full-thickness dermal round wounds in rabbit ear as judged by the size of granulation tissue area, number of capillaries, and re-epithelialization rate of the wounds. Expressions of α-smooth muscle actin (α-SMA), vascular endothelial growth factor (VEGF), and fibroblast growth factor receptor were upregulated in the wounded area injected with AdCMV-Smad3. Consistent with the *in vivo* findings, overexpression of Smad3 induced α-SMA, VEGF, and TGF-β1 expression and augmented chemotactic response in cultured dermal fibroblasts. Therefore, exogenous administration of Smad3 targeting dermal fibroblasts accelerated tissue repair in a rabbit dermal ulcer model by affecting fibroblast responses associated with wound healing. The results suggest that Smad3, when over-expressed in dermal fibroblasts, can promote wound healing.

Key words: adenovector/fibroblast/Smad7
J Invest Dermatol 123:229–236, 2004

The wound healing is a multi-step complex process consisting of inflammation, granulation tissue formation, angiogenesis, re-epithelialization, and wound contraction (Singer and Clark, 1999). When a full-thickness dermal wound is made and filled by a fibrin clot, inflammatory cells first migrate into the plasma clot and release local growth factors, such as transforming growth factor-β (TGF-β), platelet-derived growth factor (PDGF), and fibroblast growth factor (FGF), which stimulate fibroblasts from the adjacent intact dermis to migrate to the wounded site. The migrating fibroblasts, along with newly formed vessels, fill the wound, which results in the formation of granulation tissue. Activated fibroblasts differentiate into myofibroblasts, a subpopulation of specialized fibroblasts that express α-smooth muscle actin (α-SMA), which elaborate collagen and other matrix components and which eventually contract the newly formed connective tissue to bring together the edges of the wound, followed by re-epithelialization and wound closes.

TGF-β is a multi-functional cytokine involved in cellular proliferation, survival, differentiation, migration, and extracelluar matrix production (Massague, 1990). Numerous evidence suggested that exogenous administration of TGF-β into the skin accelerated wound healing, either directly or indirectly, by stimulating recruitment of inflammatory cells, the production of extracellular matrix production, the formation of new blood vessels, and wound contraction (Sporn *et al*, 1983; Roberts, 1995). For instance, the injection of TGF-β directly to the wound at the time of wounding increased the healing rate accompanied by an increased influx of mononuclear cells and fibroblasts and by marked increases in collagen deposition at the site of application of TGF-β in rats (Mustoe *et al*, 1987).

Recent investigation has revealed that the action of TGF-β is mediated mainly by the Smad family of proteins (Heldin *et al*, 1997; Attisano and Warana, 2000; Massague, 2000). Activated TGF-β receptors phosphorylate the cytosolic receptor-activated Smad2 and Smad3, which form heteromeric complexes with Smad4, and enter the nucleus, bind to DNA, and regulate gene transcription in cooperation with DNA binding cofactors. Inhibitory Smads, Smad6 and Smad7, block TGF-β signal transduction, in part, by preventing the interaction of Smad2/3 with the activated TGF-β type I receptor.

In contrast to the prediction based on therapeutic effect of ectopic TGF-β on wound healing, Smad3-deficient mice showed accelerated wound healing associated with reduction of the influx of inflammatory cells and increased re-epithelialization (Ashcroft *et al*, 1999), suggesting that

Abbreviations: α-SMA, α-smooth muscle actin; cDNA, complementary DNA; FGF, fibroblast growth factor; PDGF, platelet-derived growth factor; TGF-β, transforming growth factor-β; VEGF, vascular endothelial growth factor

endogenous Smad3 functioned inhibitory for wound healing. In this study, we investigated the effect of exogenous expression of Smad3 in dermal fibroblasts on cutaneous wound healing using a rabbit dermal ulcer model.

Results

Adenovector-mediated *in vivo* gene transfer to the skin To determine whether exogenous Smad3 regulated wound healing, we examined the effect of exogenous Smad3 or Smad7 for comparison on tissue repair in a rabbit dermal ulcer model by using adenoviral-mediated skin gene delivery. We have previously demonstrated the feasibility of *in vivo* gene transfer to the skin mediated by replication-deficient adenoviral vectors (Setoguchi *et al*, 1994b).

Consistent with the previous report, subcutaneous injection of the adenovirus-containing lacZ cDNA (AdCMV-lacZ) into the rabbit ear showed significant expression of exogenous lacZ in the skin as judged by *in situ* β-galactosidase staining 2 days after the injection (Fig 1*A*). In higher magnification of the skin, the staining was observed largely in cells with spindle morphology (fibroblasts) in the rabbit dermis (Fig 1*B*).

Immunohistochemical studies with anti-Smad3 or anti-Smad7 antibody showed that the expression of Smad3 or Smad7 was detected on day 8 post-wounding after subcutaneous injection of AdCMV-Smad3 or AdCMV-Smad7 (Fig 2). It should be noted that the antibodies used for immunohistochemical detection of Smad3 or Smad7 failed to detect endogenous Smad3 or Smad7, but detected only overexpressed Smad3 or Smad7 after adenovirus infection in the tissues.

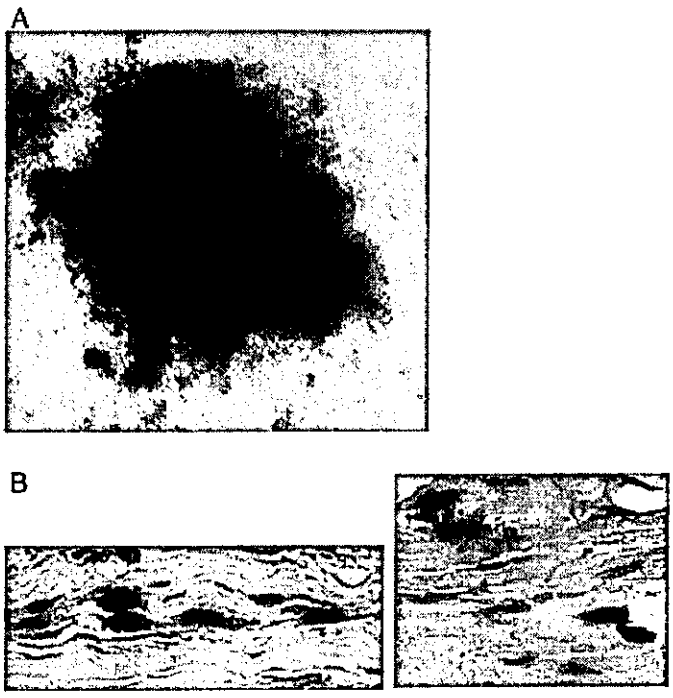

Figure 1
Expression of exogenous lacZ in rabbit skin. AdCMV-lacZ (5×10^8 pfu) was injected subcutaneously in the inner side of the ear. Two days after the injection, the skin was evaluated for the presence of the lacZ product (blue staining, β-galactosidase) using X-gal stain. Macroscopic (*A*) and microscopic (*B*) pictures of the skin subcutaneously injected with AdCMV-lacZ were shown. Please note that βgalactosidase expression (blue staining) was observed in the injected skin area (*A*) and interstitial spindle-like cells (*B*).

Exogenous Smad3, but not Smad7, accelerates cutaneous wound healing in rabbits We then examined the effect of *in vivo* gene transfer and expression of Smad3 or Smad7 on tissue repair after full-thickness wounding on rabbit ear. The amount of granulation tissue area, number of capillary lumens in the granulation tissue, and degree of re-epithelialization 8 days after the wounding were significantly enhanced in the wounded skin injected with AdCMV-Smad3 when compared with those in the wounded skin injected with AdCMV-lacZ (Fig 3). Interestingly, the injection of AdCMV-Smad3 showed a level of the wound healing equivalent to the application of total 1.5 μg of TGF-β1 (+AdCMV-lacZ) into the wounded skin. In contrast, the number of capillary lumens in the granulation tissue and degree of re-epithelialization 8 days after the incisional wounding were significantly reduced in the wounded skin injected with AdCMV-Smad7 when compared with those in the wounded skin injected with AdCMV-lacZ (Fig 3).

Because histological evaluation revealed that the injection of AdCMV-Smad3 accelerated tissue repair in a rabbit ulcer model, we next examined the effect of exogenous Smad3 on cellular and molecular events involved in wound healing. As shown in Fig 4, the number of α-smooth muscle (α-SMA) positive cells (myofibroblasts) and expression of VEGF and FGF receptors were strongly enhanced in the wounded skin injected with AdCMV-Smad3 when compared with the wounded skin injected with AdCMV-lacZ or AdCMV-Smad7. Thus, accelerated healing of dermal ulcer in a rabbit ear injected with AdCMV-Smad3 could be attributed, at least in part, to increased number of myofibroblast and increased expression of VEGF and FGF receptor in the skin.

Overexpression of Smad3 induces α-SMA, VEGF, and TGF-β1 expression and increases chemotactic response in human dermal fibroblasts *in vitro* Because exogenous administration of Smad3 affected granulation tissue formation, angiogenesis, and re-epithelialization *in vivo*, we examined the effect of Smad3 overexpression on several functions of dermal fibroblasts involved in wound healing.

Human dermal fibroblasts were infected with AdCMV-lacZ, AdCMV-Smad3, and AdCMV-Smad7 as previously described (Sumiyoshi *et al*, 2003) and evaluated for α-SMA expression, VEGF and TGF-β1 expression, and fibroblast chemotaxis (Figs 5–7). We found that overexpression of Smad3, but not lacZ or Smad7, strongly induced α-SMA expression as shown by western blotting and immunofluorescence studies (Fig 5). Overexpression of Smad3 also induced VEGF production (Fig 6*A*) and TGF-β1 expression (Fig 6*B*). In addition, fibroblast chemotaxis was augmented in human dermal fibroblasts overexpressing Smad3 when compared with the cells overexpressing lacZ or Smad7 (Fig 7). These results suggested that overexpression of Smad3 was sufficient to express α-SMA, VEGF, and TGF-β1 and to induce chemotactic response in dermal fibroblasts.

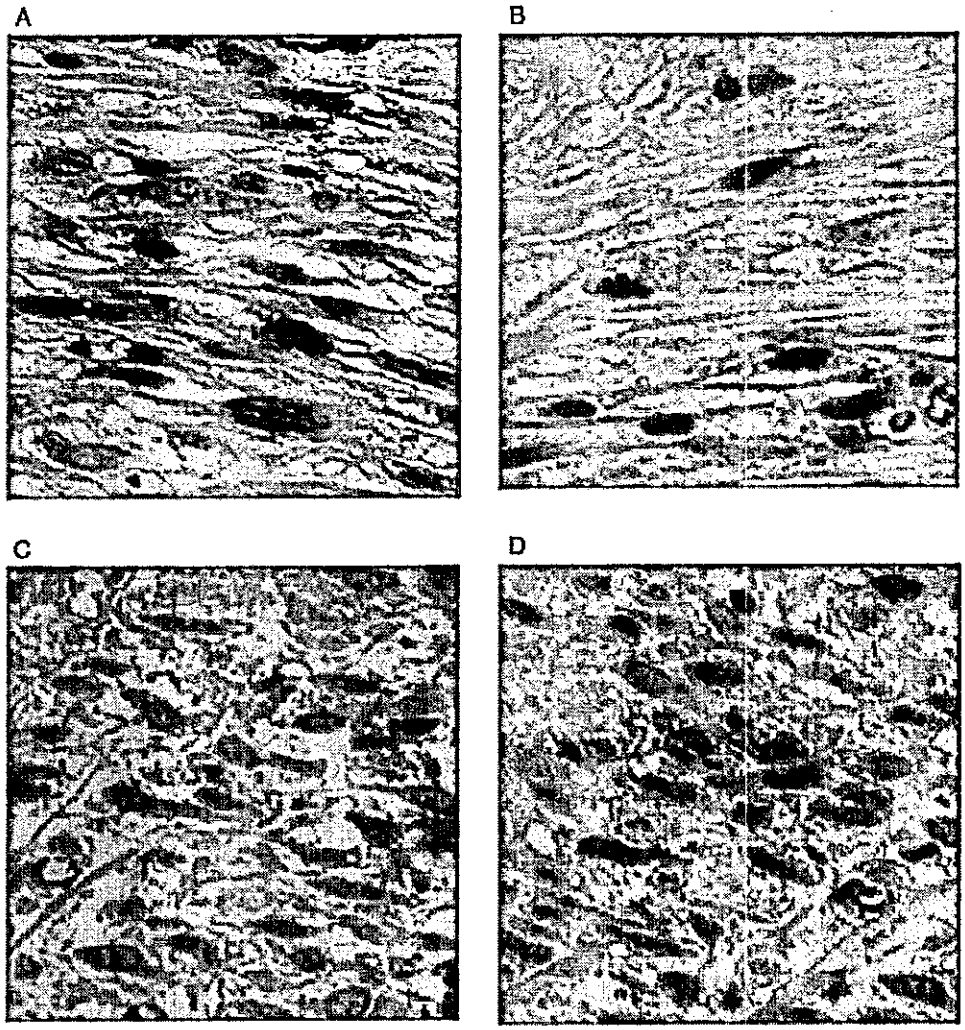

Figure 2
Expression of exogenous Smad3 or Smad7 in wounded skin. AdCMV-Smad3 (*A* and *B*) or AdCMV-Smad7 (*C* and *D*) (5×10^8 pfu) was injected subcutaneously in the inner side of the ear. Two days after the injections, full-thickness dermal round wounds were made in the injected area. On 8 days after the wounding, skin sections were immunohistochemically evaluated for the presence of Smad3 or Smad7 using antibodies against these Smads. Pictures after immunohistochemical stainings with specific antibodies against Smad3 (*A* and *C*) or against Smad7 (*B* and *D*) were shown. Brown color indicates positive staining. Please note that anti-Smad3 antibody showed immunoreactivity in the skin sections injected with AdCMV-Smad3 (*A*), but not with AdCMV-Smad7 (*C*). Please also note that anti-Smad7 antibody showed immunoreactivity in the skin sections injected with AdCMV-Smad7 (*D*), but not with AdCMV-Smad3 (*B*).

Discussion

In this study, we showed that subcutaneous injection of adenovirus-containing Smad3 cDNA into the rabbit ear accelerated tissue repair following full-thickness dermal wounds based on improvement of histological and cellular/molecular parameters (Figs 3 and 4). Because subcutaneous injection of adenoviruses-containing Smads appeared to target mainly dermal fibroblasts in our system (Figs 1 and 2, Setoguchi *et al*, 1994b), the accelerated wound healing by AdCMV-Smad3 could be, at least in part, attributed to the effect of exogenous Smad3 on several fibroblast functions involved in wound healing; that is, myofibroblast differentiation (α-SMA expression), VEGF and FGF receptors, and TGF-β1 expression, and chemotactic response as shown in Figs 5–7.

Ashcroft *et al* (1999) reported that Smad3-deficient mice showed accelerated cutaneous wound healing, suggesting that endogenous Smad3 had inhibitory effect on cutaneous wound healing. They suggested that downregulation of inflammation and acceleration of re-epithelialization of keratinocytes might contribute to the accelerated wound healing in Smad3-deficint mice. In contrast, we found that exogenous Smad3 resulted in increased granulation tissue formation and re-epithelialization (Fig 3). In Smad3-deficient mice, not only fibroblasts but also keratinocytes and inflammatory cells are Smad3-deficient and they observed net results of Smad3 deficiency in cutaneous wound healing. In our study, however, main target cells were dermal fibroblasts (Figs 1 and 2). Therefore, we think that this study emphasizes the activity of TGF-β/Smad3 on dermal fibroblast responses in the process of wound healing and the difference of target cells may explain different results in these studies. Alternatively, endogenous deficiency of Smad3 throughout the development may affect the cell function that is not attributed to the molecule itself or even alter the function of cells that do not express the molecule. This may also explain the different results in these studies. In addition, it should be noted that re-epithelialization in the whole wounded areas is usually complete between days 15 and 20 post-wounding in this dermal ulcer model in the rabbit ear and this study evaluate early phase of cutaneous wound healing regarding re-epithelialization.

Previous studies reported that dermal fibroblasts expressed α-SMA, VEGF, and FGF receptors in response to TGF-β (Kikuchi *et al*, 1992; Desmouliere *et al*, 1993; Pertovaara *et al*, 1994). Because *in vivo* expression of α-SMA, VEGF, and FGF receptors after AdCMV-Smad3 injection appeared to be confined to the interstitial fibroblast-like cells (Fig 4) and overexpression of Smad3 induced these molecules in human dermal fibroblasts

in vitro (Figs 5 and 6), it is likely that, although TGF-β activates multiple intracellular signaling pathways (Massague, 2000), "Smad3" is sufficient for mediating TGF-β-induced expression of α-SMA, VEGF, and FGF receptors in dermal fibroblasts both *in vitro* and *in vivo*.

TGF-β is a potent chemoattractant for human dermal fibroblasts (Postlethwaite *et al*, 1987). Our findings that overexpression of Smad3 in human dermal fibroblasts enhanced chemotaxis (Fig 7) and increased granulation tissue formation after AdCMV-Smad3 injection (Fig 3) suggested that Smad3 mediated fibroblast chemotaxis both *in vitro* and *in vivo*. It remains unclear, however, whether Smad3, either directly or indirectly, stimulates fibroblast chemotaxis *in vivo*.

We speculate that exogenous expression of Smad3 may have some advantages over that of TGF-β for treatment of cutaneous wounds. First, because we found that the effect of AdCMV-Smad3 on cutaneous wound healing was comparable with the effect of 1.5 μg exogenous TGF-β1 (Figs 3 and 4), exogenous expression of Smad3 may be useful for treatment of cutaneous wounds without unfavorable systemic effect of TGF-β toward other organs or systems such as tissue fibrosis and immune suppression. Secondly, recent evidence suggests that chronic wounds become unresponsiveness to growth factors including PDGF and TGF-β (Hasan *et al*, 1997; Agren *et al*, 1999), resulting in delayed or incomplete wound healing. For instance, Kim *et al* (2003) reported that fibroblasts from chronic wounds showed decreased TGF-β type II receptor expression with their lack of response to TGF-β. Thus, direct activation of intracellular TGF-β signaling by overexpression of Smad3 may be a useful way for treatment of chronic cutaneous wounds even if dermal fibroblasts in wounded areas have altered TGF-β receptor expression and lack of TGF-β response.

In summary, we showed that exogenous overexpression of Smad3 in dermal fibroblasts promoted cutaneous wound healing. Our findings suggest that modulation of Smad3 expression in dermal fibroblasts may have therapeutic potential for the treatment of cutaneous wounds.

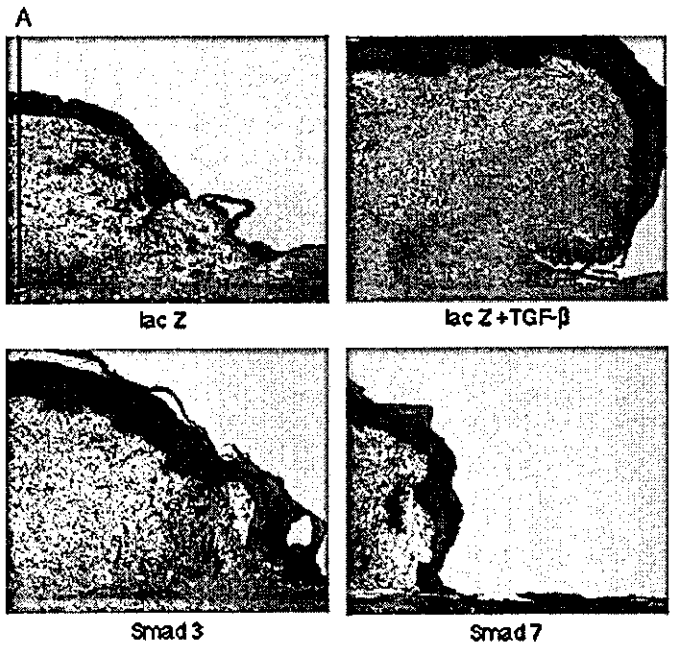

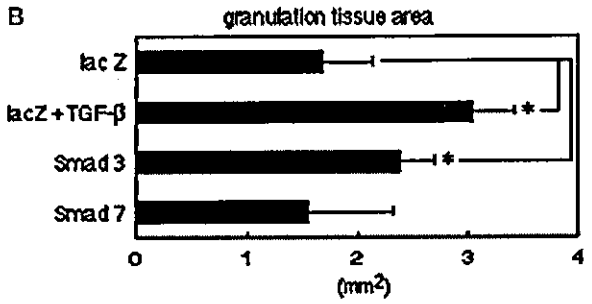

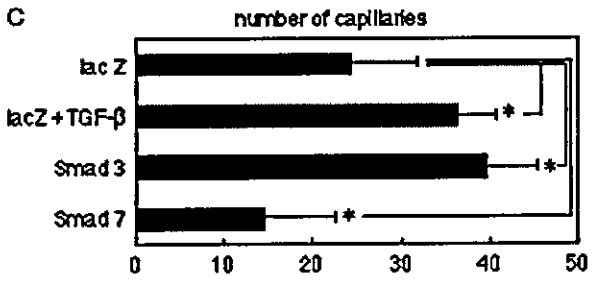

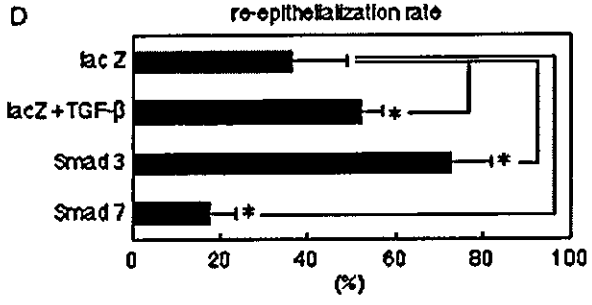

Materials and Methods

Adenovirus vector construction and virus purification The recombinant E1-deleted adenoviral vectors carrying mouse Smad3, Smad7, or lacZ complementary DNA (cDNA) under cytomegarovirus promoters, AdCMV-Smad3, AdCMV-Smad7, or AdCMV-lacZ, were generated, purified, and transfected as previously described (Setoguchi *et al*, 1994a; Fujii *et al*, 1999).

***In situ* β-galactosidase staining** *In situ* β-galactosidase staining was performed using *in situ* β-galactosidase staining kit (STRATAGENE) according to the manufacture's instruction.

The rabbit ear dermal ulcer model Wounding design and sample preparation were performed according to the previously reported method (Tsuboi *et al*, 1995). Female white rabbits, 2.5–3.0 kg (Shiraishi Laboratory Animals, Tokyo, Japan) were anesthetized

Figure 3
Acceleration of cutaneous wound healing by exogenous Smad3, but not Smad7. AdCMV-lacZ, AdCMV-Smad3, or AdCMV-Smad7 was subcutaneously injected into rabbit skin. Two days after the injections, full-thickness dermal round wounds were made in the injected area with or without application of TGF-β1 as indicated. Eight days after the wounding, skin sections were microscopically evaluated by HE staining (*A*) and by quantitative analysis of granulation tissue area (*B*), the number of capillaries (*C*), and re-epithelialization rate (*D*) as described in the Materials and Methods. Please note that injection of AdCMV-Smad3 enhanced granulation tissue area (*B*), the number of capillaries (*C*), and re-epithelialization rate as compared with injection of AdCMV-lacZ. The arrow in figure A lacZ picture indicates the wounded area in rabbit skin.

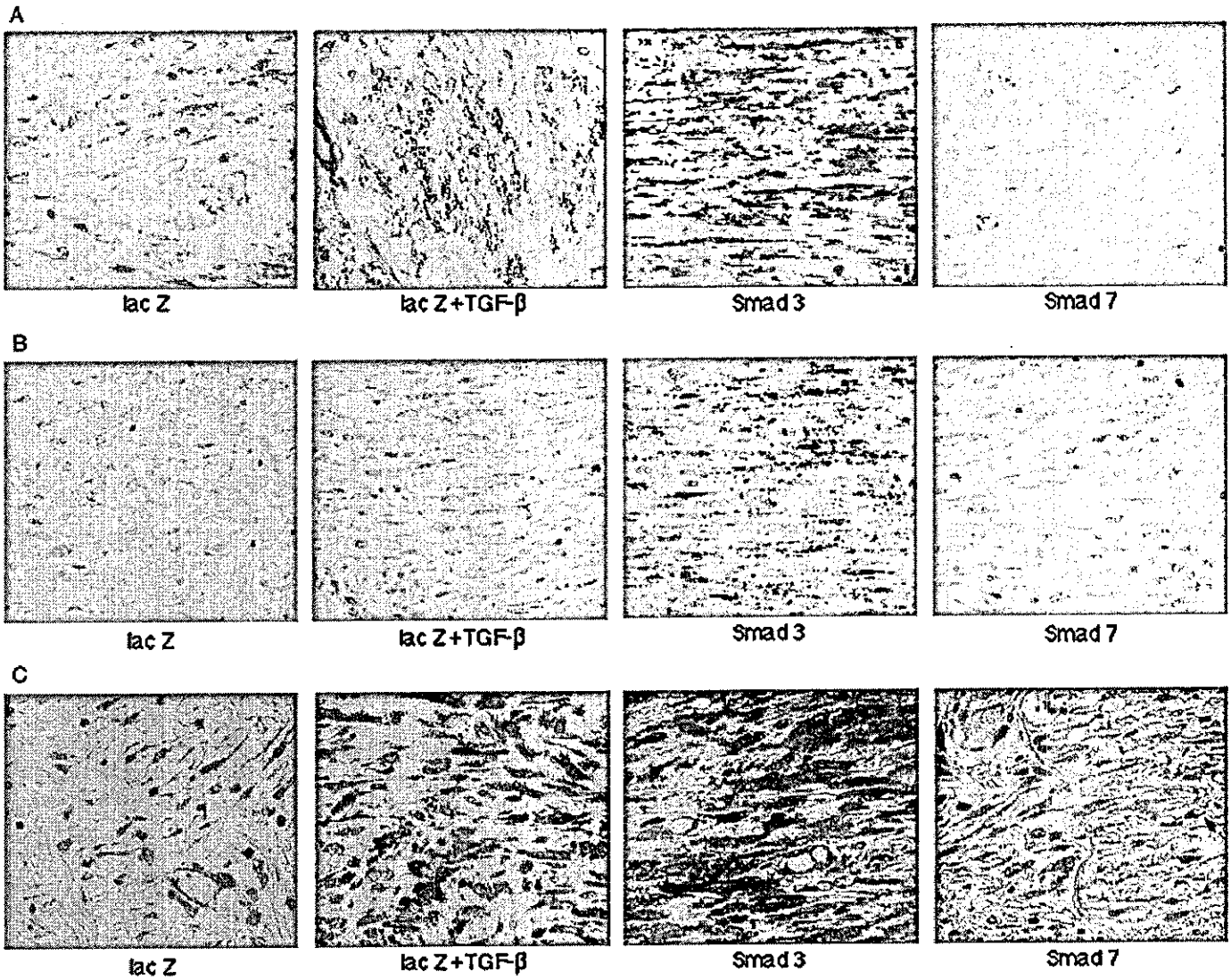

Figure 4
Induction of α-SMA, VEGF, and FGF receptor expression by exogenous Smad3 in wounded skin. AdCMV-lacZ, AdCMV-Smad3, or AdCMV-Smad7 was subcutaneously injected into rabbit skin. Two days after the injections, full-thickness dermal round wounds were made in the injected area with or without application of TGF-β1 as indicated. Eight days after the wounding, skin sections were immunohistochemically stained with antibodies specific for α-SMA (*A*), VEGF (*B*), and FGF receptor (*C*). Brown color indicates the positive staining. Please note that injection of AdCMV-Smad3 enhanced α-SMA (*A*), VEGF (*B*), and FGF receptor (*C*) expression (brown color) in the wounded skin.

with xylazine hydrochloride solution (10 mg per kg) (Bayer Co., Leverkusen, Germany) and ketamine hydrochloride solution (30 mg per kg) (Sankyo Co., Tokyo, Japan). After sterilization with iodine and alcohol, 5×10^8 plaque-forming units (pfu) of AdCMV-lacZ, AdCMV-Smad3, or AdCMV-Smad7 were injected subcutaneously in the inner side of the rabbit ear. The doses and timing of the adenovirus injection were determined according to our previous study (Setoguchi *et al*, 1994b). Forty-eight hours after the injections, four full-thickness round wounds were prepared on the injected area using a calibrated 6 mm trephine (Acu Punch, Acuderm Inc., Lauderdale, Florida) under sterile conditions (day 1). The perichondrium was kept undamaged. The wounds were covered with a sterilized transparent dressing (Tegaderm, 3M, Tokyo, Japan), and 20 μL PBS or 20 μL recombinant human TGF-β1 (R&D, Minnesota) solution (25 ng per μL: 500 ng per one ulcer) was applied to each wound using a syringe once every other day until the 5th day (on day 1, 3, and 5; total 1.5 μg per one ulcer). The ear was bandaged and kept covered throughout the experiment. The rabbits were killed on the 8th day after the wounding by intravenous administration of pentobarbital solution. The wounded areas were excised and fixed in 10% buffered formalin solution. All animal experiments were performed according to the approved manual of the Institutional Review Board of Juntendo University.

Histological evaluation After overnight fixation, the tissue was trimmed and cut through at the widest margin. The tissue was embedded in paraffin and sectioned in 5 μm increments. The sections were made perpendicular to the anterior–posterior axes and perpendicular to the surface of the wound. Three sections were placed on a slide, and stained with hematoxylin and eosin. Of the three sections on any one slide, the section with the widest original wound margin was used for assessment. The parameters measured were degree of granulation tissue area, number of capillaries, and re-epithelialization as previously described (Tsuboi *et al*, 1995). Each of the parameters was graded numerically as described below.

Granulation tissue area The amount of granulation tissue was quantified by measuring the area of granulation tissue (mm^2) in the section perpendicular to the surface of the wound. Granulation tissue was traced by a computerized morphometric analysis (KS-400, Carl Zeiss Inc., Gotingen, Germany).

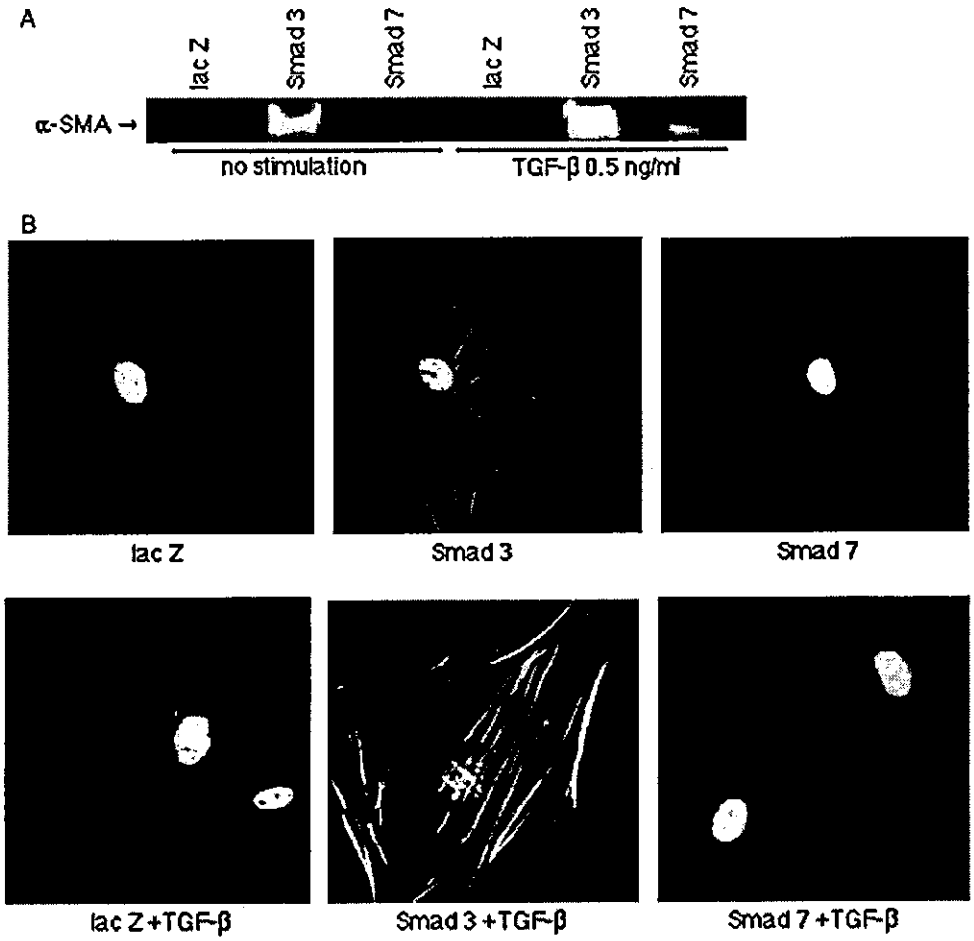

Figure 5
Induction of α-SMA by overexpression of Smad3 in human dermal fibroblasts. Cultured human dermal fibroblasts infected with adenoviruses carrying lacZ, Smad3, or Smad7 cDNA were incubated with 0.5 (*A*) or 10 ng per mL (*B*) of TGF-β1 for 24 h. Then, western blot analysis (*A*) or immunofluorescence anlayisis with anti-α-SMA antibody followed by incubation with Alexa488-conjugated secondary antibody (Green staining) (*B*) was performed. Nucleus was stained with DAPI solution (Blue staining). Similar results were obtained in at least three independent experiments. Please note that overexpression of Smad3 in dermal fibroblasts enhanced α-SMA expression as judged by western blotting (*A*) and immunofluorescence study (*B*).

Number of capillaries The number of capillary lumens in the granulation tissue was counted in the complete wound cross-section at × 100 magnification.

Re-epithelialization The degree of re-epithelialization was measured by a computerized morphometric analysis (KS-400) and was given a value by percentage; 0% was equivalent to no closure and 100% was equivalent to complete wound closure.

Immunohistochemistry Skin paraffin sections were deparaffinized and then preincubated with normal mouse or goat serum (1:20) for 20 min. The slides were incubated overnight at 4°C with mouse monoclonal antibody against vascular endothelial growth factor (VEGF) (05-443, Upstate Biotechnology, Lake Placid, New York 1:50) or mouse monoclonal antibody against FGF receptor (MAB125, CHEMICON, Temecula, California 1:150), goat polyclonal antibody against Smad3 (sc-6202, Santa Cruz Biotechnology, Inc., Santa Cruz, California 1:100), mouse monoclonal antibody against α-SMA (U7033, DAKO EPOS, 1:1), or goat polyclonal antibody against Smad7 (sc-7004, Santa Cruz Biotechnology, Inc., 1:100). Sections were then incubated for 60 min at room temperature with an Envision labeled polymer reagent (K1490, DAKO, Glostrup, Denmark). To increase their sensitivity, sections were then incubated for 10 min at room temperature with a Tyramide signal amplification (TSA) Biotin System (NEN life science products, Boston, Texas, 1:50). Sections were then incubated with a streptavidin (DAKO, 1:400) for 30 min. Between steps, the slides were rinsed for 10 min in PBS. All sections were lightly counterstained with hematoxylin.

Cell culture Primary human dermal fibroblasts were cultured as previously described (Lee *et al*, 1996). Briefly, fibroblasts were obtained from the outgrowth of infant foreskin and maintained in Dulbecco's modified Eagle's medium (DMEM) supplemented with 10% fetal calf serum (FCS) and 100 μg per mL streptomycin. All experiments were carried out using fibroblasts in passage 4–8th. Infection of recombinant adenoviruses was performed at a multiplicity of infection (m.o.i.) of 2×10^2 pfu per cell in 1 mL of serum-free DMEM for 60 min and overexpression of exogenous Smad3 or Smad7 in the cultured human dermal fibroblasts after the transfection was previously reported (Sumiyoshi *et al*, 2003). Dermal fibroblasts infected with the adenovirus solutions were cultured in DMEM supplemented with 10% FCS for 48 h and thereafter used for the following experiments.

Immunoblot Immunoblotting with anti-α-SMA antibody (American Research Product, Belmont, Massachusetts 1:500) was performed as previously described (Nakao *et al*, 1997).

Immunofluorescence microscopy Dermal fibroblasts infected with the adenovirus solutions were grown on rat tail collagen type I-coated eight well culture slides (Beckton Dickinsons Labware, Bedford, Massachusetts) in the absence or presence of TGF-β1 (10 ng per mL) (R&D, Minnesota) for 24 h, then washed with PBS and fixed with 4% paraformaldehyde. Following permeabilization, slides were stained with anti-α-SMA antibody (American Research Product, 1:3) diluted in PBS 90 min at room temperature. After extensive washing, slides were incubated with Alexa488-conjugated goat anti-mouse antibody (1:200) for 1 h at room temperature. After extensive washing, slides were incubated with DAPI solution (100 ng per mL) for 5 min. Fibroblasts were mounted in fluorescent mounting medium (DAKO), and images were acquired using a confocal microscopy (ECLIPSE E800, Nikon, Japan).

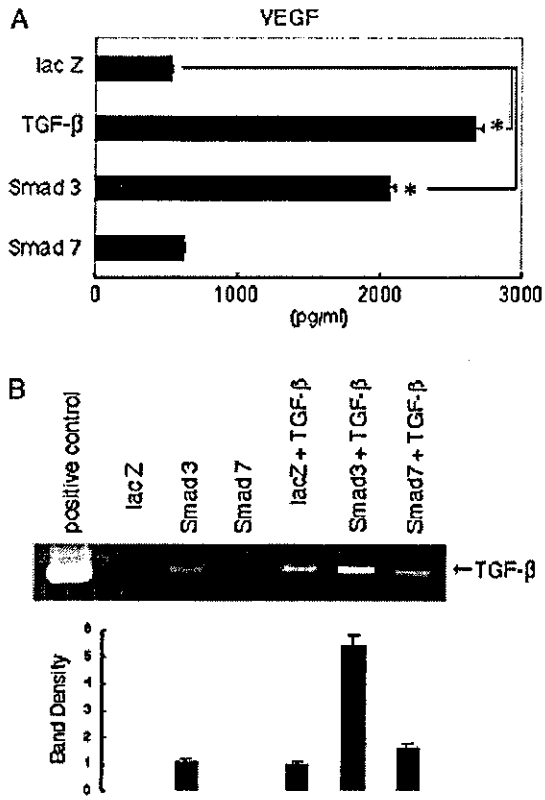

Figure 6
Induction of VEGF and TGF-β1 by overexpression of Smad3 in human dermal fibroblasts. Cultured human dermal fibroblasts infected with adenoviruses carrying lacZ, Smad3, or Smad7 cDNA were incubated with 10 ng per mL of TGF-β1 for 72 h. Then, human VEGF concentration in the culture supernatants was measured by ELISA (*A*) or mRNAs were taken for detection of TGF-β1 mRNA by RT-PCR (*B*). The relative density of the each PCR band from three separate experiments was estimated by using a one-dimensional image analyzer and was indicated as a bar graph. Data are indicated as the mean ± SD. Please note that overexpression of Smad3 in dermal fibroblasts enhanced VEGF (*A*) and TGF-β1 (*B*) expression.

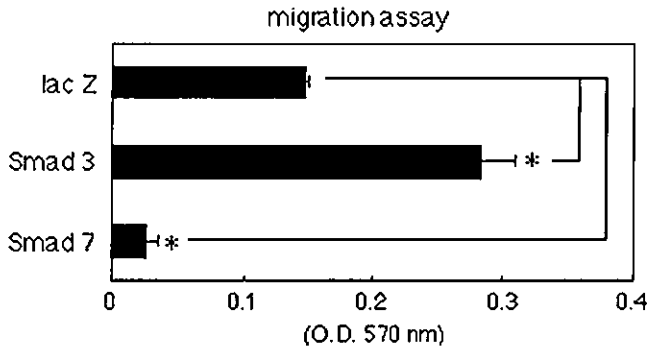

Figure 7
Enhanced migration of human dermal fibroblasts by overexpression of Smad3. Cultured human dermal fibroblasts infected with adenoviruses carrying lacZ, Smad3, or Smad7 cDNA were subjected to migration assay as described in the Materials and Methods. Data are indicated as the mean ± SD of triplicate samples. *$p<0.05$, significantly different from the mean value of the corresponding control response. Similar results were obtained in at least three independent experiments. Please note that overexpression of Smad3 in dermal fibroblasts enhanced their migration.

Migration assay Migration assay was performed using quantitative cell migration assay kit (ECM500, Chemicon International Inc.) according to the manufacture's instruction.

Cytokine ELISA The amount of VEGF in the culture supernatant of fibroblasts was determined using human VEGF ELISA kit (R&D, Minnesota).

RT-PCR Total RNA was prepared from cultures of dermal fibroblasts 72 h after the infection of adenoviruses carrying lacZ, Smad3, and Smad7, as recommended by manufacture's instructions for Isogen solution (Nippon Gene, Japan). cDNA was synthesized from 3 μg of total RNA using first strand cDNA synthesis kit (Ready To Go) (Amersham Pharmacia, Piscataway, New Jersey). PCR amplification (95°C for 1 min, 58°C for 2 min, and 72°C for 2 min; 25 cycles) was performed in a DNA thermal cycler (Perkin-Elmer, Wellesley, Massachusetts). The PCR products were size-fractionated by agarose gel electrophoresis using 2.0% agarose, and stained with 0.5 μg per mL ethidium bromide. As positive controls, we used expression constructs of human TGF-β1 cDNA. Primers used in this study were as follows: TGF-β1 (5′-AGTATGGACACAGGCTCTCC-3′ and 3′-GTCTTATGGCTTCC-GTCTG-5′), and hypoxanthine phosphoribosyltransferase (HPRT) (5′-TTCTTTGCTGACCTGCTG-3′ and 3′-TTTCTACCAGTTCCAG-CG-5′).

Data analysis Data are summarized as mean ± SD. Statistical analysis was performed using the unpaired Student *t* test. $p<0.05$ was considered to be significant.

We thank Drs Kazuko Yokomizo, Atsushi Furuhata, Toshinari Funaki, Yuko Kikuchi, Hiroko Ushio, Chiharu Nishiyama, Keiko Maeda, Toshiro Takai, Tomoko Tokura for discussion and technical assistance, and M. Matsumoto and E. Kawasaki for secretarial assistance. This work was supported in part by the grant from the Ministry of Education, Culture, Sports, Science, and Technology, Japan and from the Ministry of Health, Labor, and Welfare, Japan.

DOI: 10.1111/j.0022-202X.2004.22730.x

Manuscript received October 7, 2003; revised March 3, 2004; accepted for publication March 8, 2004

Address correspondence to: Atsuhito Nakao, Department of Immunology, Faculty of Medicine, University of Yamanashi, 1110, Shimokato, Tamaho, Yamanashi 409-3898, Japan. Email: anakao@yamanashi.ac.jp

References

Agren MS, Steenfos HH, Dabelsteen S, Hansen JB, Dabelsteen E: Proliferation and mitogenic response to PDGF-BB of fibroblasts isolated from chronic venous leg ulcers is ulcer-age dependent. J Invest Dermatol 112:463–469, 1999

Ashcroft GS, Yang X, Glick A, *et al*: Mice lacking Smad3 show accelerated wound healing and an impaired local inflammatory response. Nature Cell Biol 1:260–266, 1999

Attisano L, Warana JL: Smads as transcriptional co-modulators. Curr Opin Cell Biol 12:235–243, 2000

Desmouliere A, Geinoz A, Gabbiani F, Gabbiani G: Transforming growth factor-β1 induces α-smooth muscle actin expression in graulation tissue myofibroblasts and in quiescent and growing cultured fibroblasts. J Cell Biol 122:103–111, 1993

Fujii M, Takeda K, Imamura T, *et al*: Roles of bone morphogenetic protein type I receptors and Smad proteins in osteoblast and chondroblast differentiation. Mol Bio Cell 10:3801–3813, 1999

Hasan A, Murata H, Falabella A, Ochoa S, Zhou L, Badiavas E, Falanga V: Dermal fibroblasts from venous ulcers are unresponsiveness to the action of transforming growth factor-β1. J Dermatol Sci 16:59–66, 1997

Heldin CH, Miyazono K, Ten Dijke P: TGF-β signaling from cell membrane to nucleus through SMAD proteins. Nature 390:465–471, 1997

Kikuchi K, Yamakage A, Smith EA, LeRoy EC, Trojanowska M: Differential modulation of bFGF receptors by TGF-β in adult skin, scleroderma skin, and newborn foreskin fibroblasts. J Invest Dermatol 99:201–205, 1992

Kim BC, Kim HT, Park SH, Cha JS, Yufit T, Kim SJ, Falanga V: Fibroblasts from chronic wounds show altered TGF-β-signaling and decreased TGF-β type II receptor expression. J Cell Physiol 195:331–336, 2003

Lee YR, Oshita Y, Tsuboi R, Ogawa H: Combination of insulin-like growth factor (IGF)-1 and IGF-binding protein-1 promotes fibroblast-embedded collagen gel contraction. Endocrinology 137:5278–5283, 1996

Massague J: The transforming growth factor-β family. Annu Rev Cell Biol 6:597–641, 1990

Massague J: How cells read TGF-β signals. Nat Rev Mol Cell Biol 1:169–178, 2000

Mustoe TA, Pierce GF, Thomason A, Gramates P, Sporn MB, Deuel TF: Accelerated healing of incisional wounds in rats induced by transforming growth factor-β. Science 237:1333–1336, 1987

Nakao A, Imamura T, Souchelnytskyi S, *et al*: TGF-β receptor-mediated signaling through Smad2, Smad3, and Smad4. EMBO J 16:5353–5362, 1997

Pertovaara L, Kaipainen A, Mustonen T, Orpana A, Ferrara N, Saksela O, Alitalo K: Vascular endothelial growth factor is induced in response to transforming growth factor-β in fibroblastic and epithelial cells. J Biol Chem 269:6271–6274, 1994

Postlethwaite AE, Keski-Oja J, Moses HL, Kang AH: Stimulation of the chemotactic migration of human fibroblasts by transforming growth factor-β. J Exp Med 165:251–256, 1987

Roberts AB: Transforming growth factor-β: Activity and efficacy in animal models of wound healing. Wound Rep Reg 3:408–418, 1995

Setoguchi Y, Danel C, Crystal RG: Stimulation of erythropoiesis by *in vivo* gene therapy: Physiologic consequences of transfer of the human eythropoietin gene to experimental animals using an adenovirus vector. Blood 84:2953–2964, 1994a

Setoguchi Y, Jaffe HA, Danel C, Cystal RG: *Ex vivo* and *in vivo* gene transfer to the skin using replication-deficient recombinant adenovirus vectors. J Invest Dermatol 102:415–421, 1994b

Singer AJ, Clark RAF: Cutaneous wound healing. New Eng J Med 341:738–746, 1999

Sporn MB, Robers AB, Shull JH, Smith JM, Ward JM, Sodek J: Polypeptide transforming growth factors isolated from bovine sources and used for wound healing *in vivo*. Science 219:1329–1331, 1983

Sumiyoshi K, Nakao A, Setoguchi Y, Okumura K, Tsuboi R, Ogawa H: Smads regulate collagen gel contraction by human dermal fibroblasts. Br J Dermatol 149:464–470, 2003

Tsuboi R, Shi CM, Sato C, Cox GN, Ogawa H: Co-administration of insulin-like growth factor (IGF)-I and IGF-binding protein-1 stimulates wound healing in animal models. J Invest Dermatol 104:199–203, 1995

Available online at www.sciencedirect.com
SCIENCE DIRECT®
Biochemical and Biophysical Research Communications 315 (2004) 240–245
BBRC
www.elsevier.com/locate/ybbrc

Oxidative stress reduces histone deacetylase 2 activity and enhances IL-8 gene expression: role of tyrosine nitration

K. Ito, T. Hanazawa, K. Tomita, P.J. Barnes, and I.M. Adcock*

Department of Thoracic Medicine, National Heart and Lung Institute, Imperial College London, Dovehouse Street, London SW3 6LY, UK

Received 6 January 2004

Abstract

Oxidative stress is a characteristic of chronic inflammatory diseases. The reactive oxygen intermediate hydrogen peroxide (H_2O_2) is an important signaling molecule that modulates gene expression. We have demonstrated that H_2O_2 significantly enhanced cytokine production in BEAS-2B cells, with a maximal effect at 4 h. This did not result from enhanced NF-κB activation, but through decreased activity of histone deacetylase (HDAC)2. This results in increased inflammatory gene expression following acetylation of specific histone residues. Decreased HDAC2 activity was associated with tyrosine nitration status. Peroxynitrite and SIN-1, a peroxynitrite generator, were also able to reduce HDAC2 activity via tyrosine nitration. Our data suggest that oxidative stress contributes to worsening inflammation via reduction of HDAC2 activity through HDAC2 nitration. This novel mechanism of inflammation may be important in increasing the severity and chronicity of inflammatory diseases.

Keywords: Oxidative stress; Histone acetylation; Gene expression; Inflammation; Peroxynitrite

Oxidative stress is characteristic of chronic inflammatory diseases such as asthma, chronic obstructive pulmonary disease (COPD), rheumatoid arthritis, and inflammatory bowel disease [1,2]. Elevated intracellular reactive oxygen species (ROS) are generated under various physiological and pathological conditions, including inflammation, ischemia and reperfusion, and sepsis. They can be derived from sources as different as activated inflammatory cells, oxidized lipoproteins, cigarette smoke, and structural cells [3]. Major ROS are superoxide anions (O^{2-}), hydroxyl radicals (·OH), and H_2O_2. In addition, peroxynitrite is a potent radical formed from a rapid interaction between superoxide anions (O^{2-}) and nitric oxide (NO) [4]. ROS mediate some biological responses, such as cytokine (IL-6, IL-8, and TNFα) induction by IL-1β or TNFα [4,5]. This is reported to be due to enhanced NF-κB activation in response to H_2O_2 [4–6].

Chromatin structure and binding of proteins to DNA can be modulated by reversible acetylation of lysine residues within the N-terminal tails of core histones. In the resting cell, DNA is tightly compacted to prevent transcription factor accessibility. During activation of the cell, this compact inaccessible DNA is made available to transcription factors through histone acetylation. This chemical modification is carried out by histone acetyltransferases (HAT) and counteracted by histone deacetylases (HDAC) [7] and [8] many transcriptional co-activators, such as CREB-binding protein (CBP), have intrinsic HAT activity. IL-1β and TNFα can both stimulate the binding of NF-κB (p65 subunit) to CBP, increase HAT activity, and induce histone acetylation, thus leading to increased inflammatory gene (such as GM-CSF and IL-8) transcription [9,10]. Hydrogen peroxide (H_2O_2) and other ROS can also induce enhanced inflammatory mediator release from cells, a process that is associated with changes in histone acetylation [11].

Several reports have shown that HDACs 1–3 can also be associated with inactive p65 and play a role in the regulation of NF-κB-mediated gene transcription without altering the degree of DNA binding [9,12–14]. Thus, changes in HDAC activity associated with p65 can enhance or repress NF-κB-mediated gene expression [12].

* Corresponding author Fax: +44-207-351-5675.
E-mail address: ian.adcock@imperial.ac.uk (I.M. Adcock).

0006-291X/$ - see front matter © 2004 Elsevier Inc. All rights reserved.
doi:10.1016/j.bbrc.2004.01.046

We have previously reported that HDAC2 expression and activity is decreased in smokers, COPD subjects, and mild asthma patients and that there is a good correlation between cytokine production and HDAC activity in alveolar macrophages from smokers and nonsmokers [11]. Reduced HDAC2 may be a key factor in the development of inflammation in airway obstructive disease. There is abundant evidence for increased oxidative stress and peroxynitrite formation in COPD and severe asthma [2]. We show that nitration of HDAC2 following oxidative stress may account for the reduced HDAC activity seen in cells from patients with oxidant stress related diseases.

Materials and methods

Materials. Thirty percentage of H_2O_2 and *N*-acetyl-L-cysteine (NAC) were purchased from Sigma (Sigma, Poole, UK); IL-1β was from R&D (Abingdon, UK); DCFH-DA and SIN-1 were from Molecular Probes (Leiden, Netherlands); and peroxynitrite was from Cayman Chemicals (Ann Arbor, MI, USA). Anti-p65 (sc-109, sc-7151), anti-phosphotyrosine (sc-508), anti-HDAC2 (sc-7899), and anti-HDAC1 (sc-6298) antibodies were obtained from Santa Cruz Biotec (Santa Cruz, California, USA), and anti-nitrotyrosine (1A6) was obtained from Upstate (Charlottesville, VA, USA).

Cell culture. BEAS-2B cells were grown to 50% confluence in keratinocyte conditioned medium (Gibco, Paisley, UK). Before experimentation, cells were serum-starved for 24 h in medium without EGF and bovine pituitary extracts. Cells were stimulated by IL-1β (1 ng/ml) in the presence or absence of H_2O_2 (100 μM) or SIN-1 (500 μM).

Cytokine ELISA. Determination of GM-CSF and IL-8 expression was measured by sandwich ELISA (R&D Systems Europe, Abingdon, UK) according to the manufacturer's instructions.

DCF assay for oxidative stress. Oxidative stress was detected by the modified method described by Wang and Joseph [15]. Viable cells were plated into 96-well culture plates 1 day before the experiments. On the day of the experiments, after removing the medium, the cells in the plates were washed with Krebs–Ringer–Hepes–glucose–glutamine buffer (KRH buffer) and then incubated with 100 μM of 2′,7′-dichlorofluorescin diacetate (DCFH-DA) in the loading medium in 5% CO_2/95% air at 37 °C for 30 min. After DCFH-DA was removed, the cells were washed and incubated with KRH buffer with SIN-1 (500 μM) or H_2O_2 (100 μM) and the fluorescence of the cells from each well was measured and recorded. The excitation filter was set at 485 nm and the emission filter was set at 530 nm.

Nuclear extraction. Cells were collected and resuspended in mild lysis buffer [10 mM Tris–HCl, pH 8.0, 150 mM NaCl, 0.5% NP-40, and complete protease inhibitor cocktail (Boehringer–Mannheim)] for 10 min. Nuclei were collected by microcentrifugation (10,000 rpm, 5 min, 4 °C) and resuspended in Tris-based high salt buffer (10 mM Tris–HCl, pH 8.0, 500 mM NaCl, 0.25 mM EDTA, 10 mM of 2-mercaptoethanol, and complete protease inhibitor cocktail). After 30 min, supernatant was collected and diluted with Tris-based, no salt buffer (10 mM Tris–HCl, pH 8.0, 0.25 mM EDTA, 10 mM of 2-mercaptoethanol, and complete protease inhibitor cocktail) to 40 mM NaCl final concentration.

Immunoprecipitation. Extracts were prepared using 100 μl of modified RIPA buffer [50 mM Tris–HCl, pH 8.0, 150 mM NaCl, 1.0% Triton X-100, 0.5% NP-40, 0.1% SDS, 0.5% deoxycholate, and complete protease inhibitor cocktail (Boehringer–Mannheim)] as previously described [9]. For the HDAC assay, immunoprecipitates were washed twice with HDAC buffer (10 mM Tris–HCl, pH 8.0, 20 mM NaCl, 0.25 mM EDTA, and 10 mM of 2-mercaptoethanol) and for Western blotting the buffer was aspirated completely and resuspended in Laemmli buffer.

Western blotting. Immunoprecipitates or nuclear extractions were analyzed by SDS–PAGE and Western blot analysis using ECL as previously described [9].

NF-κB activation. NF-κB activation was measured with TransAM NF-κB kit (Active Motif, California, USA).

Histone deacetylase assay. HDAC assays were performed as previously described [9].

Immunocytochemistry. BEAS-2B cells (0.5×10^6) were cultured in 8-well slide chambers with IL-1β (1 ng/ml) in the presence or absence of H_2O_2 and immunocytochemistry for p65 performed as previously described [9]. Stained cells were observed by confocal microscopy. Confocal scanning laser microscopy images were collected with a Leica confocal microscope, equipped with a 488/514 nm dual band argon ion laser. An oil-immersion objective was used and images were collected using TCSNT software.

Chromatin immunoprecipitation (ChIP) assay. BEAS-2B cells pretreated with H_2O_2 (4 h) or trichostatin A (TSA, 10 min) were treated with IL-1β (1 ng/ml) as described above. After a 0.5-h incubation, protein–DNA complexes were fixed by formaldehyde (1% final concentration) and treated as previously described [9]. Acetylated H4 or NF-κB–p65 binding IL-8 promoter (−121 to +61) was quantified by real-time PCR using a QuantiTect SYBR Green PCR kit (Qiagen) on a Rotor-Gene 3000 (Corbett Research, NSW, Australia).

Statistics. Results are expressed as means ± standard error of the mean (SEM). A multiple comparison was made between the mean of the control and the means from each individual treatment group by Dunnett's test using SAS/STAT software (SAS Institute, Cary, NC, USA). All statistical testing was performed using a two-sided 5% level of significance.

Results

H_2O_2 enhances IL-1β-stimulated cytokine expression

Pretreatment of human airway epithelial cells (BEAS2B) with H_2O_2 (100 μM) for 4 h slightly enhanced basal IL-8 production but markedly potentiated IL-1β-stimulated IL-8 production (2497 ± 226 ng/ml versus 1066 ± 64) (Fig. 1A) without affecting cell survival (data not shown). This enhancement by pretreatment of H_2O_2 was maximal at 4 h (Fig. 1B). Four hour pretreatment of H_2O_2 also enhanced GM-CSF production as well as IL-8 (211 ± 22 vs 138 ± 36). This effect was blocked by the anti-oxidant *N*-acetyl-L-cysteine (NAC, 10 mM, Fig. 1C) (IL-1β only 1066 ± 64, IL-1β + H_2O_2, 2497 ± 226, and IL-1β + H_2O_2 + NAC 1334 ± 09 ng/ml).

H_2O_2 does not enhance NF-κB nuclear translocation

IL-1β-induced p65 nuclear translocation was rapid (detectable at 10 min), peaked at 30 min, and remained elevated for at least 2 h (data not shown). H_2O_2 (100 μM) induced some p65 nuclear translocation but this was minimal compared to that seen with IL-1β and peaked at 2 h (Fig. 2A). H_2O_2 did not significantly enhance IL-1β-induced p65 nuclear translocation (Fig. 2B). These results were confirmed by immunocytochemistry (Fig. 2C). Furthermore, H_2O_2 did not

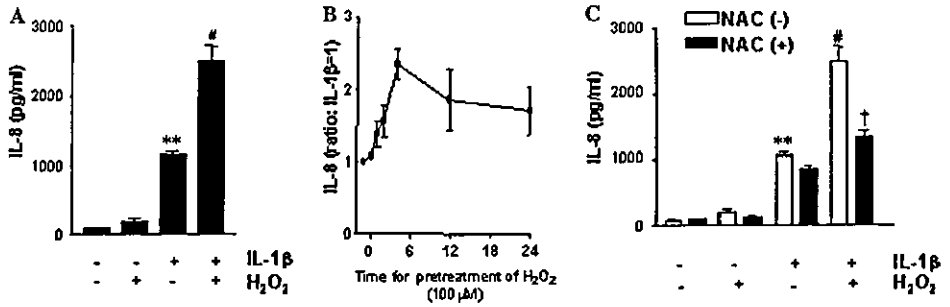

Fig. 1. Effect of H_2O_2 on IL-1β-induced inflammatory cytokine production. (A) BEAS-2B cells were stimulated by IL-1β (1 ng/ml) for 24 h in the presence or absence of H_2O_2 (100 μM) and IL-8 was measured by ELISA. (B) Effect of different pretreatment periods with H_2O_2 on IL-1β-induced IL-8 production. (C) The effect of *N*-acetyl-L-cysteine (10 mM) added 10 min before H_2O_2 pretreatment. Cells were stimulated with IL-1β 4 h after treatment and IL-8 was measured after overnight incubation. Results are expressed as means ± SEM ($n = 3$–5), $^*p < 0.05$, $^{**}p < 0.01$ compared with control; $^\#p < 0.05$ compared with IL-1β-stimulated; and $^\dagger p < 0.05$ compared with IL-1β plus H_2O_2.

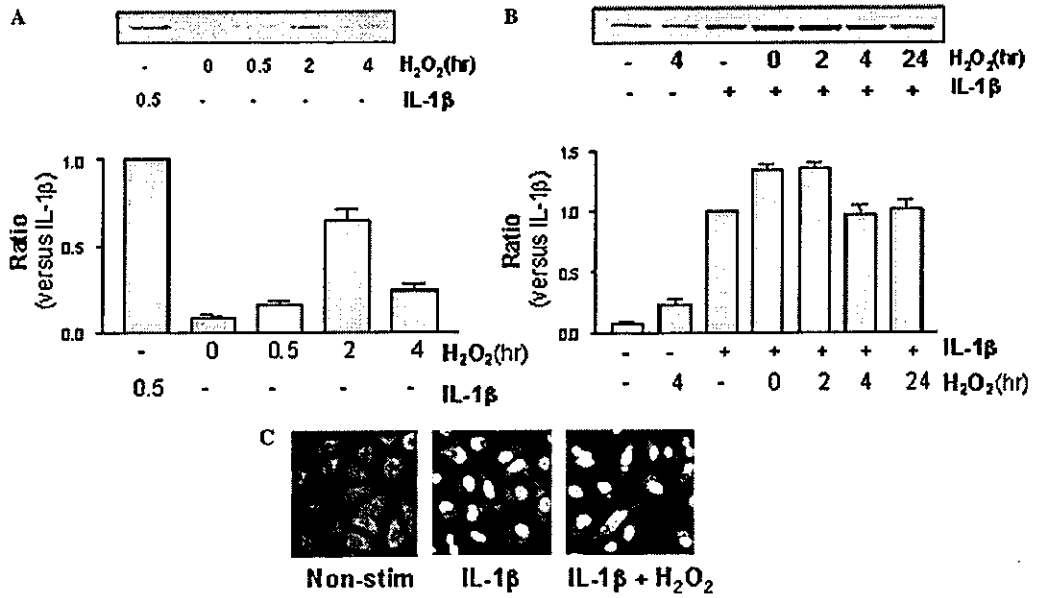

Fig. 2. H_2O_2 does not markedly enhance IL-1β-induced NF-κB nuclear translocation. (A) Representative Western blot analysis of NF-κB p65 subunit nuclear translocation in BEAS-2B cells. The cells were treated with IL-1 (1 ng/ml) or H_2O_2 (100 μM) and collected at the indicated time (h). Densitometric analysis of each band is plotted below. Results are expressed as means ± SEM as the ratio versus IL-1β alone, $n = 3$ independent experiments. (B) Representative Western blot analysis of NF-κB p65 subunit nuclear translocation in BEAS-2B cells treated with IL-1β (1 ng/ml) in the presence of H_2O_2 (100 μM). H_2O_2 was pretreated for indicated time. Cells were collected 30 min after IL-1β stimulation. Densitometric analysis of each band is plotted below. Results are expressed as means ± SEM as the ratio versus IL-1β alone. (C) Immunocytochemistry of p65 in BEAS-2B cells. Cells were pre-treated with H_2O_2 for 4 h and fixed 30 min after IL-1β stimulation.

significantly enhance IL-1β induced p65 activation measured with TransAM kit (absorbance: basal, 0.21 ± 0.045; IL-1β, 1.43 ± 0.16; and IL-1β + H_2O_2, 1.58 ± 0.16). Trichostatin A (10 ng/ml), a histone deacetylase inhibitor, also enhanced IL-1β-induced IL-8 production (2821 ± 171 vs. 1066 ± 64 ng/ml) without activation of NF-κB (data not shown). Pathways, other than NF-κB activation, must therefore be responsible for the marked elevation of IL-1β-stimulated cytokine release.

H_2O_2 enhances GM-CSF promoter-associated histone acetylation

We analyzed the effect of H_2O_2 (100 μM) on IL-1β-induced increase in histone 4 acetylation associated with the IL-8 promoter in BEAS-2B cells by quantitative chromatin immunoprecipitation. Following IL-1β treatment p65 immunoprecipitates showed a marked enrichment of IL-8 promoter (−121 to +61) DNA (Fig. 3A). Immunoprecipitation with an antibody

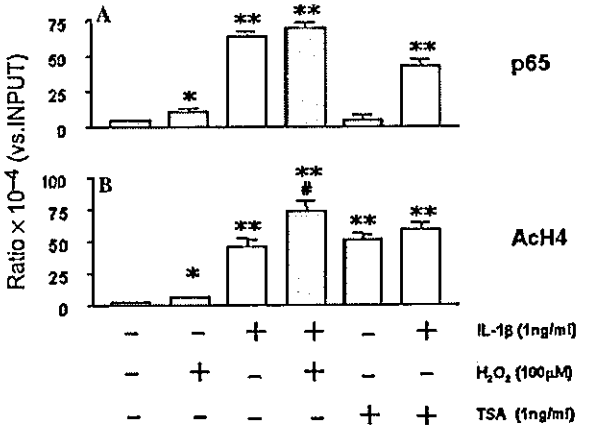

Fig. 3. Chromatin immunoprecipitation assay shows that H_2O_2 does not enhance p65 DNA binding but increases histone H4 acetylation at the IL-8 promoter. BEAS-2B cells were pretreated with H_2O_2 (100 μM) for 4 h before incubation with IL-1β (1 ng/ml). After 30 min, proteins and DNA were cross-linked by formaldehyde treatment and chromatin pellets were extracted. Following sonication, NF-κB p65 subunit (A) and acetylated histone H4 (B) were immunoprecipitated and the associated DNA was amplified by PCR. Results are representative of three independent experiments. $^*p < 0.05$, $^{**}p < 0.01$ compared with control; $^\#p < 0.05$ compared with IL-1-stimulated.

against acetylated histone 4 resulted in the enrichment for the DNA segments encompassing the GM-CSF promoter following IL-1β treatment (Fig. 3B). H_2O_2 did not effect IL-1β-induced enrichment of p65-associated IL-8 promoter fragments but caused an enhancement in the enrichment of acetylated H4-associated IL-8 promoter fragments (Fig. 3). This suggests that enhanced histone acetylation at the NF-κB site is related to either enhanced HAT activity or reduced HDAC activity.

H_2O_2 represses HDAC activity and expression

Pretreatment with H_2O_2 (100 μM, 4 h) reduced basal HDAC activity (330 ± 15 versus 499 ± 91 dpm/μg protein) and inhibited IL-1β-stimulated HDAC activity (487 ± 20 versus 898 ± 64 dpm/μg protein) (Fig. 4A). This effect occurred prior to changes in HDAC2 protein expression since H_2O_2 decreased HDAC2 expression only after 24 h (Fig. 4b). This effect of H_2O_2 was concentration-dependent and reached plateau at 100 μM (Fig. 4C).

Oxidative stress inhibits HDAC activity

IL-1β induced tyrosine phosphorylation of HDAC2, which was associated with a concomitant increase of HDAC activity (data not shown). This IL-1β-induced increase in HDAC2 activity was inhibited by alkaline phosphatase pre-treatment (basal, 381 ± 84; IL-1β, 667 ± 140; IL-1β + alkaline phosphatase, 410 ± 94 dpm/μg protein).

H_2O_2 induced nitration of HDAC2 from 0.5 h after stimulation, which peaked at 4 h, and was still elevated at 24 h (Fig. 5A). Peroxynitrite (500 nM) also enhanced tyrosine nitration of HDAC2 but this did not affect basal HDAC2 activity, but inhibited IL-1β-stimulated HDAC activity (Fig. 5B). Furthermore, SIN-1 (500 μM), a peroxynitrite generator, did not affect basal HDAC activity but significantly ameliorated the IL-1β-induced HDAC2 activity (basal, 107 ± 12; SIN-1, 76 ± 8; IL-1β, 165 ± 7; and IL-1β + SIN-1, 76 ± 6 dpm/μg protein) (Fig. 5C). This correlated with the ability of SIN-1 to enhance IL-1β-induced IL-8 production (2196 ± 22 versus 1091 ± 89 ng/ml) (Fig. 5C). SIN-1 also

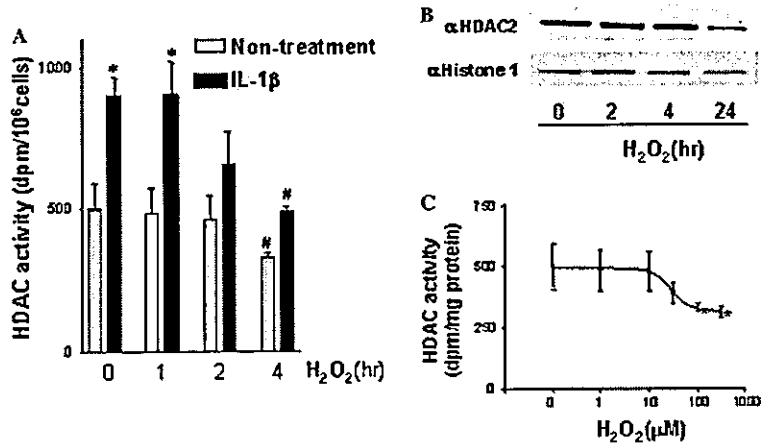

Fig. 4. Time- and concentration-dependent effect of H_2O_2 on HDAC activity and expression. (A) H_2O_2 (100 μM) directly inhibits HDAC activity in BEAS-2B cells at 4 h. Cells were collected at 1 h after IL-1β (1 ng/ml) stimulation, nuclear protein was extracted, and total HDAC activity was measured using [^{3}H]acetate incorporated histone. Results are expressed as means ± SEM for three experiments. $^*p < 0.05$ compared to control; $^\#p < 0.05$ compared to $t = 0$. (B) Western blot analysis of HDAC2 in nuclear extracts of BEAS-2B cells shows decreased expression following H_2O_2 (100 μM) stimulation for 24 h. Histone 1 protein expression was detected as control. (C) Concentration-dependent inhibition of HDAC activity by H_2O_2 after 4 h incubation. $^*p < 0.05$ compared to control

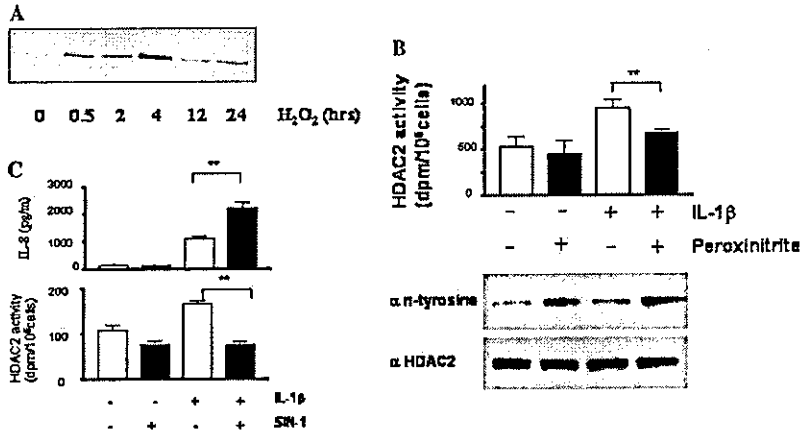

Fig. 5. H_2O_2 and peroxynitrite induce HDAC2 tyrosine nitration and suppression of HDAC activity. (A) Western blotting analysis of H_2O_2-induced tyrosine nitration of HDAC2 in BEAS-2B cells. Cells were collected after the indicated time, HDAC2 immunoprecipitated, and nitrotyrosine levels were determined. (B) Peroxynitrite directly regulates HDAC2 activity and nitration. Cells were stimulated with IL-1β (1 ng/ml) or control medium and after 1 h were collected, lysed with immunoprecipitation buffer, and immunoprecipitated with anti-HDAC2 antibody. Peroxynitrite (500 nM) was incubated with the immunoprecipitates from IL-1β-treated or non-treated cells for 10 min at 30 °C. HDAC activity assay and Western blotting for nitro-tyrosine and HDAC2 protein were performed. Results are expressed as means ± SEM ($n = 3$). $^{**}p < 0.01$ compared to IL-1β-stimulation. (C) SIN-1 (500 μM) attenuates HDAC2 immunoprecipitated HDAC2 activity and enhanced IL-8 production. Results are expressed as means ± SEM ($n = 3$). $^{**}p < 0.01$ compared to IL-1β-stimulation.

decreased HDAC1 and HDAC3 activity by 71% and 65% of IL-1β-induced HDAC activity, respectively. H_2O_2 (100 μM) and SIN-1 (500 μM) produced peroxynitrite at 3.6 ± -0.65 and 17.4 ± 0.61 μM, respectively.

Discussion

In this study we have demonstrated that H_2O_2 and peroxynitrite enhanced IL-1β-induced expression of inflammatory cytokines, such as GM-CSF and IL-8. This effect could be blocked by the anti-oxidant NAC. Using chromatin immunoprecipitation assays in cells treated with IL-1β plus H_2O_2, the IL-8 promoter region was associated with much greater levels of acetylated histone H4 than those after IL-1β stimulation alone. Under the same conditions, there was no change in p65-associated IL-8 promoter suggesting no increased NF-κB DNA binding at this time. A lack of enhancement of NF-κB activation was confirmed by Western blotting, immunocytochemistry, and DNA binding activity assay (TransAM).

H_2O_2 alone reduced HDAC2 activity after 4 h but its expression reduced only at 24 h or longer. H_2O_2 also reduced IL-1β-stimulated HDAC activity at 4 h-pretreatment and the reduction in total HDAC activity correlated with the enhancement of IL-1β-induced cytokine production. At this time point there was no reduction in HDAC expression, suggesting that a post-translational modification of HDAC is involved in attenuating HDAC activity. These data suggested that enhancement of IL-1β-induced cytokine production by H_2O_2 is not associated with NF-κB activation, but with enhancement of histone acetylation by inhibition of HDAC2 activity.

Peroxynitrite, the product of the reaction between nitric oxide (NO) and superoxide anions, is a much stronger oxidant than NO or H_2O_2. As well as having a strong cytotoxic effect [2], it is also reported to change protein function via the nitration of the *ortho*-position of tyrosine residues. For example, peroxynitrite-mediated nitration of a single tyrosine residue in the cell cycle kinase cdc2 prevents tyrosine phosphorylation in endothelial cells [16]. In addition, peroxynitrite-induced nitration of tyrosine residue of EGF receptor prevents their dimerization [17]. Peroxynitrite-mediated nitration of tyrosine residues has also been shown to inactivate the mitochondrial Mn superoxide dismutase [18], the lipid aggregatory activity of surfactant protein A [19], and glutamine synthetase activity [20]. In our system, nitration of HDAC inhibited the phosphorylation-associated increase in HDAC activity induced by IL-1β (data not shown) and confirm previous data showing that enhanced HDAC activity is associated with phosphorylation [21]. This initial increase in HDAC activity may be associated with a feedback resolution of gene transcription [22]. H_2O_2 nitrated HDAC2, which is peaked at 4 h. This correlated with the HDAC activity and enhancement of IL-1β-induced cytokine production. SIN-1, a peroxynitrite generator, gave the same effect as peroxynitrite. In these cells we obtained similar levels of peroxynitrite formation with SIN-1 and H_2O_2 possibly due to the low endogenous levels of cNOS present in the cells since iNOS is not induced until much later time points [23]. Further experiments using mass

spectrometry and peptide fingerprinting are required to determine whether nitration of distinct tyrosine residues antagonizes the enhanced HDAC activity associated with phosphorylated tyrosine residues.

Neutrophils, eosinophils, and alveolar macrophage produce ROS and nitric oxide, which interact to produce peroxynitrite. Nitro-tyrosine, which is a footprint of peroxynitrite formation, is increased in COPD and bronchial asthma [2]. Reduction in HDAC activity by oxidative stress might be one of the factors that worsen inflammatory disease.

In summary, we have shown in vitro ROS enhanced IL-1β-induced inflammatory cytokine release by reduction of HDAC activity acting via tyrosine nitration. This is a novel mechanism for the enhancement of inflammation. These studies suggest that there is a potential to develop novel therapeutic agents with improved anti-inflammatory properties that have improved HDAC activation properties and highlight the potential for anti-oxidant therapy in the treatment of chronic inflammatory diseases.

Acknowledgments

This work was funded by the British Lung Foundation, the Clinical Research Committee (Royal Brompton Hospital), and GlaxoSmithKline plc (UK).

References

[1] L.S. Greene, J. Am. Coll. Nutr. 14 (1995) 317–324.
[2] I. Rahman, Curr. Drug Targets Inflamm. Allergy 1 (2002) 291–315.
[3] M. Meyer, H.L. Pahl, P.A. Baeuerle, Chem. Biol. Interact. 91 (1994) 91–100.
[4] I. Rahman, W. Macnee, Eur. Respir. J. 16 (2000) 534–554.
[5] V. Lakshminarayanan, E.A. Drab-Weiss, K.A. Roebuck, J. Biol. Chem. 273 (1998) 32670–32678.
[6] T. Shono, M. Ono, H. Izumi, S.I. Jimi, K. Matsushima, T. Okamoto, K. Kohno, M. Kuwano, Mol. Cell. Biol. 16 (1996) 4231–4239.
[7] S.Y. Roth, C.D. Allis, Cell 87 (1996) 5–8.
[8] F.D. Urnov, A.P. Wolffe, Oncogene 20 (2001) 2991–3006.
[9] K. Ito, P.J. Barnes, I.M. Adcock, Mol. Cell. Biol. 20 (2000) 6891–6903.
[10] K. Ito, E. Jazrawi, B. Cosio, P.J. Barnes, I.M. Adcock, J. Biol. Chem. 276 (2001) 30208–30215.
[11] K. Ito, S. Lim, G. Caramori, K.F. Chung, P.J. Barnes, I.M. Adcock, FASEB J. 15 (2001) 1110–1112.
[12] H. Zhong, M.J. May, E. Jimi, S. Ghosh, Mol. Cell 9 (2002) 625–636.
[13] B.P. Ashburner, S.D. Westerheide, A.S. Baldwin Jr., Mol. Cell. Biol. 21 (2001) 7065–7077.
[14] L. Chen, W. Fischle, E. Verdin, W.C. Greene, Science 293 (2001) 1653–1657.
[15] H. Wang, J.A. Joseph, Free Radic. Biol. Med. 27 (1999) 612–616.
[16] S.K. Kong, M.B. Yim, E.R. Stadtman, P.B. Chock, Proc. Natl. Acad. Sci. USA 93 (1996) 3377–3382.
[17] A. van der Vliet, M. Hristova, C.E. Cross, J.P. Eiserich, T. Goldkorn, J. Biol. Chem. 273 (1998) 31860–31866.
[18] H. Ischiropoulos, L. Zhu, J. Chen, M. Tsai, J. Martin, C. Smith, J.S. Beckman, Arch. Biochem. Biophys. 298 (1992) 437.
[19] I.Y. Haddad, H. Ischiropoulos, B.A. Holm, J.S. Beckman, J.R. Baker, S. Matalon, Am. J. Physiol. 265 (1993) L555–L564.
[20] B.S. Berlett, B. Friguet, M.B. Yim, P.B. Chock, E.R. Stadtman, Proc. Natl. Acad. Sci. USA 93 (1996) 1776–1780.
[21] M.K. Pflum, J.K. Tong, W.S. Lane, S.L. Schreiber, J. Biol. Chem. 276 (2001) 47733–47741.
[22] K. Ito, I.M. Adcock, Mol. Biotechnol. 20 (2002) 99–106.
[23] R.A. Robbins, P.J. Barnes, D.R. Springall, J.B. Warren, O.J. Kwon, L.D. Buttery, A.J. Wilson, D.A. Geller, J.M. Polak, Biochem. Biophys. Res. Commun. 203 (1994) 209–218.

Available online at www.sciencedirect.com
SCIENCE DIRECT®
Biochemical and Biophysical Research Communications 318 (2004) 422–427
BBRC
www.elsevier.com/locate/ybbrc

TWEAK/Fn14 interaction stimulates human bronchial epithelial cells to produce IL-8 and GM-CSF

Hongri Xu,[a,b] Atsushi Okamoto,[a,b] Jiro Ichikawa,[a] Takashi Ando,[a] Kachio Tasaka,[a] Keisuke Masuyama,[b] Hideoki Ogawa,[c] Hideo Yagita,[d] Ko Okumura,[d] and Atsuhito Nakao[a,c,*]

[a] *Department of Immunology, Faculty of Medicine, University of Yamanashi, Yamanashi 409-3898, Japan*
[b] *Department of Otorhinolaryngology, Head and Neck Surgery, Faculty of Medicine, University of Yamanashi, Yamanashi 409-3898, Japan*
[c] *Atopy Research Center, Juntendo University School of Medicine, Tokyo 113-8421, Japan*
[d] *Department of Immunology, Juntendo University School of Medicine, Tokyo 113-8421, Japan*

Received 17 March 2004
Available online 16 April 2004

Abstract

TNF-like weak inducer of apoptosis (TWEAK), a member of the tumor necrosis factor (TNF) family, is a multifunctional cytokine that regulates cellular proliferation, angiogenesis, inflammation, and apoptosis. In this study, we investigated the effect of TWEAK on human bronchial epithelial cells. A human bronchial epithelial cell line, BEAS2B, expressed a TWEAK receptor, fibroblast growth factor-inducible 14 (Fn14), and produced IL-8 and GM-CSF upon TWEAK stimulation in a dose-dependent manner, which was abrogated by anti-Fn14 blocking antibody. TWEAK induced phosphorylation of IκBα and BAY11-7082, a selective inhibitor of IκBα phosphorylation, inhibited the TWEAK-induced IL-8 and GM-CSF production by BEAS2B cells. Moreover, primary cultured human bronchial epithelial cells also expressed Fn14 and produced IL-8 and GM-CSF upon TWEAK stimulation. Collectively, TWEAK stimulated human bronchial epithelial cells to produce IL-8 and GM-CSF through Fn14. Because IL-8 and GM-CSF are associated with inflammatory conditions, these results suggest that TWEAK/Fn14 interaction may play some roles in airway inflammatory responses.

Keywords: TWEAK; Fn14; IL-8; GM-CSF; Bronchial epithelial cell; IκBα

TNF-like weak inducer of apoptosis (TWEAK) was first identified as a new member of the tumor necrosis factor (TNF) superfamily which induced cell death in some tumor cell lines [1]. However, recent studies have revealed that TWEAK is a multifunctional cytokine that regulates cellular proliferation, angiogenesis, and inflammation [2]. TWEAK not only induced cell death in certain tumor cell lines [3,4], but also induced proliferation of endothelial cells and angiogenesis [5], upregulated cell surface expression of adhesion molecules and induced secretion of chemokines such as IL-8 and MCP-1 in human umbilical vein endothelial cells [6], and induced IL-8, IP-10, and RANTES in human dermal fibroblasts and synoviocytes [7].

The human TWEAK gene is expressed in many different cell types and encodes for a ~30 kDa type II transmembrane protein that can be cleaved to generate an ~18 kDa soluble factor with biological activity [2]. Recently, Wiley et al. [8] have identified fibroblast growth factor-inducible 14 (Fn14) as a TWEAK receptor with physiological affinity. Fn14 is a type I transmembrane protein composed of only one cysteine-rich domain in the extracellular region and a short cytoplasmic region containing a TRAF-binding motif [9]. Saitoh et al. [10] recently reported that TWEAK stimulated two NF-κB signaling pathways; IκBα phosphorylation and p100 processing via TRAF molecules. These findings suggest that NF-κB pathway mediates TWEAK/Fn14 signaling.

* Corresponding author. Fax: +81-55-273-9542.
E-mail address: anakao@yamanashi.ac.jp (A. Nakao).

0006-291X/$ - see front matter © 2004 Elsevier Inc. All rights reserved.
doi:10.1016/j.bbrc.2004.04.036

In this study, we investigated Fn14 expression on human bronchial epithelial cells and examined the effect of TWEAK on chemokine/cytokine production by human bronchial epithelial cells. We found that TWEAK stimulated human bronchial epithelial cells to produce IL-8 and GM-CSF via Fn14. The results suggest that TWEAK/Fn14 interaction may contribute to the development of airway inflammatory responses through production of proinflammatory IL-8 and GM-CSF by bronchial epithelial cells.

Materials and methods

Reagents. Recombinant human TWEAK was purchased from Alexis Biochemicals (San Diego, CA). Anti-human Fn14 monoclonal antibodies (mAbs) (ITEM-1 and ITEM-2) were generated in our laboratory as previously described [11]. ITEM-2 is a blocking antibody preventing the interaction between TWEAK and Fn14 [11]. A selective inhibitor of IκBα phosphorylation, BAY11-7082, was purchased from Calbiochem (La Jolla, CA).

Cell culture. A human bronchial epithelial cell line, BEAS2B [12], was maintained in F-12 nutrient mixture medium (HAM) with L-glutamine (Gibco/Invitrogen, Carlsbad, CA) supplemented with 10% fetal calf serum (FCS) and 100 μg/ml streptomycin. Normal human bronchial epithelial cells were purchased from BioWhittaker/Clonetics (Walkersvile, MD) and cultured in serum-free bronchial epithelial cell growth medium, SABM (BioWhittaker/Clonetics, Walkersvile, MD), containing epidermal growth factor (EGF) (0.5 ng/ml), insulin (5 μg/ml), hydrocortisone (0.5 μg/ml), epinephrine (5 μg/ml), transferrin (10 μg/ml), retinoic acid (0.1 ng/ml), triiodothyronine (6.5 ng/ml), BSA-FAF (0.5 mg/ml), gentamicin (50 μg/ml), amphotericin B (50 ng/ml), and bovine brain pituitary extract (30 μg/ml) at 37 °C in humidified atmosphere in presence of 5% CO_2. The experiments were carried out using the cells at third or fourth passage.

Flow cytometric analysis for Fn14 expression. Cells (1×10^6) were incubated with biotinylated anti-human Fn14 mAb (ITEM-1) for 1 h at 4 °C, followed by PE-labeled avidin (BD Pharmingen, San Diego, CA). After washing with PBS, the cells were analyzed on a FACSCalibur (BD, San Jose, CA) and the data were analyzed by using the CellQuest program (BD).

ELISA. BEAS2B cells or normal human bronchial epithelial cells (1×10^6/well) were stimulated with recombinant human TWEAK or, in some experiments, with recombinant human TNF-α (R&D, Minneapolis, MN), for the indicated time period and the concentrations of human IL-8, TARC, Eotaxin, and GM-CSF in the culture supernatants of the cell cultures were determined by using the ELISA kits (R&D, Minneapolis, MN) according to the manufacturer's instruction. In some experiments, 10 μg/ml anti-human Fn14 mAb (ITEM-2) or isotype-matched control Ig, or 2 μM of BAY11-7082, was added in the cell cultures 1 h before the addition of TWEAK. This dose of BAY11-7082 did not affect cell viability and inhibited IκBα phosphorylation in our preliminary experiments and previous literatures [13,14].

Western blot. BEAS2B cells stimulated with recombinant human TWEAK (100 ng/ml) for the indicated time periods were suspended in RIPA buffer (20 mM Tris–HCl (pH 8.0), 137 mM NaCl, 1 mM $MgCl_2$, 1 mM $CaCl_2$, 10% glycerol, 1% Nonidet P-40, 0.5% deoxycholate, and 0.1% SDS) supplemented with 0.1 mM phenylmethylsulfonyl fluoride, 100 μM Na_3VO_4, and 20 mM β-glycerophosphate. Extracts were cleared by centrifugation. Whole cell extracts (10 μg) were fractionated on 9–15% SDS–polyacrylamide gels and transferred onto immobilon-P membrane. Immunoblotting was performed using the phosphoPlus IκBα (Ser32) antibody kit (Cell Signaling Technology, Beverly, MA, USA) according to the manufacturer's instruction or using antibodies against phosphorylated (Ser536) or non-phosphorylated NF-κB p65 (Cell Signaling Technology, Beverly, MA, USA).

Data analysis. Data are summarized as means ± SD of triplicate samples. Statistical analysis was performed by the unpaired Student's *t* test. A value of $P < 0.05$ was considered to be significant.

Results

A human bronchial epithelial cell line, BEAS2B, expresses Fn14

To determine whether TWEAK can act on human bronchial epithelial cells, we first examined the expression of Fn14 on a human bronchial epithelial cell line, BEAS2B. Flow cytometric analysis using anti-Fn14 mAb [11] showed a higher fluorescence from cells incubated with anti-Fn14 mAb compared to those incubated with control antibody (Fig. 1), indicating that Fn14 was significantly expressed on the cell surface.

TWEAK induces IL-8 and GM-CSF production by BEAS2B cells

Since BEAS2B cells expressed Fn14, we then investigated whether TWEAK could stimulate BEAS2B cells through Fn14. Human bronchial epithelial cells are known to produce several chemokines/cytokines associated with inflammation such as IL-8 and GM-CSF upon various stimuli [15]. We thus examined the effect of recombinant TWEAK on IL-8 and GM-CSF production by BEAS2B cells. As shown in Figs. 2A and B, TWEAK induced IL-8 production in a dose- or time-dependent manner, which was almost completely inhibited by blocking the TWEAK/Fn14 interaction with anti-Fn14 mAb (Fig. 2C). We also found that

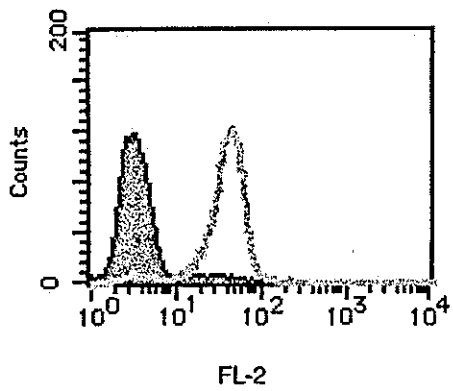

Fig. 1. Cell surface expression of Fn14 on BEAS2B cells. BEAS2B cells were stained with biotinylated anti-human Fn14 mAb (open histogram) or control Ig (filled histogram), followed by PE-labeled avidin, and then analyzed by flow cytometry. A representative of three repeated experiments with similar results is shown.

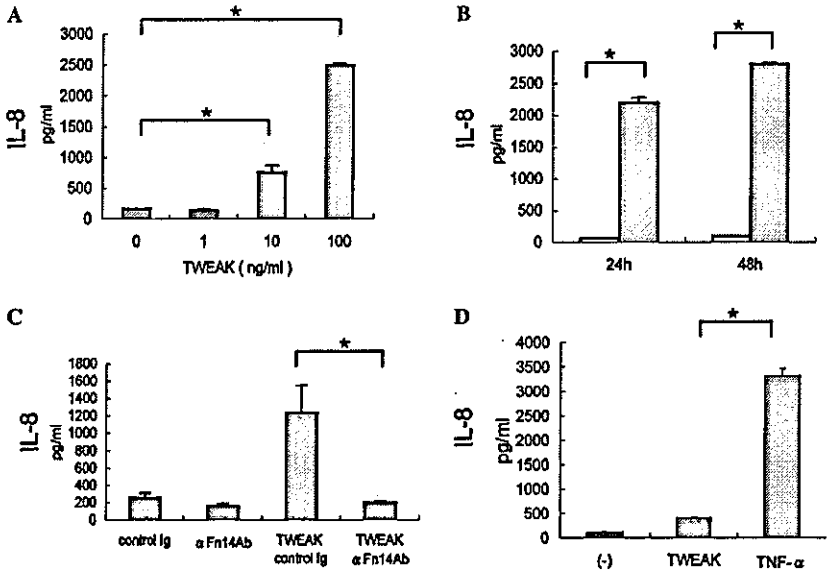

Fig. 2. Tweak induces IL-8 production by BEAS2B cells via Fn14. BEAS2B cells were stimulated with the indicated doses of TWEAK for 48 h (A) or stimulated with 100 ng/ml TWEAK for 24 or 48 h (B), or stimulated with 10 ng/ml TWEAK for 48 h in the presence of 10 μg/ml anti-Fn14 blocking mAb or control Ig (C) or stimulated with 10 ng/ml TWEAK or 10 ng/ml TNF-α for 48 h (D). Human IL-8 concentration in the culture supernatant was measured by ELISA. Data are indicated as means ± SD of triplicate samples. $^*p < 0.05$. Similar results were obtained in three repeated experiments.

TWEAK induced GM-CSF production by BEAS2B cells, which was again inhibited by anti-Fn14 mAb (Figs. 3A and B). No significant production of MCP-1, TARC, or Eotaxin was observed upon TWEAK stimulation of BEAS2B cells (data not shown). The IL-8 and GM-CSF production induced by TWEAK was significantly less than that induced by TNF-α (Figs. 2D and 3C). These findings indicated that TWEAK stimulated BEAS2B cells to produce IL-8 and GM-CSF via Fn14.

Phosphorylation of IκBα is critical for TWEAK-induced IL-8 and GM-CSF production by BEAS2B cells

To explore the mechanisms by which TWEAK stimulated BEAS2B cells, we investigated IκBα phosphorylation in TWEAK-stimulated BEAS2B cells. Saitoh et al. [10] showed that TWEAK induced phosphorylation of IκBα, resulting in NF-κB activation in fibroblasts. As shown in Fig. 4A, we found that TWEAK induced phosphorylation of IκBα and also NF-κB p65 at 20–60 min after the stimulation in BEAS2B cells. Moreover, a selective inhibitor of IκBα phosphorylation, BAY11-7082, substantially inhibited TWEAK-induced IL-8 and GM-CSF production by BEAS2B cells (Fig. 4B). These results suggested that phosphorylation of IκBα was critical for TWEAK-induced IL-8 and GM-CSF production by BEAS2B cells.

Primary cultured human bronchial epithelial cells express Fn14 and produce IL-8 and GM-CSF upon TWEAK stimulation

In order to address the physiological relevance, we examined the effect of recombinant human TWEAK on primary cultured human bronchial epithelial cells. We found that normal human bronchial epithelial cells expressed Fn14 and produced IL-8 and GM-CSF upon TWEAK stimulation (Fig. 5). These results indicated that TWEAK induced IL-8 and GM-CSF production not only in an immortalized bronchial epithelial cell line (BEAS2B) but also in primary cultured bronchial epithelial cells.

Discussion

In this study, we demonstrated that TWEAK induced IL-8 and GM-CSF production by BEAS2B cells through Fn14 expressed on their surface (Figs. 1–3). Phosphorylation of IκBα was critical for the TWEAK-induced IL-8 and GM-CSF production by BEAS2B cells (Fig. 4). In addition, not only BEAS2B cells but also primary cultured human bronchial epithelial cells expressed Fn14 and produced IL-8 and GM-CSF upon TWEAK stimulation (Fig. 5). These findings suggest that TWEAK/Fn14 interaction stimulates human bronchial epithelial cells to produce proinflammatory

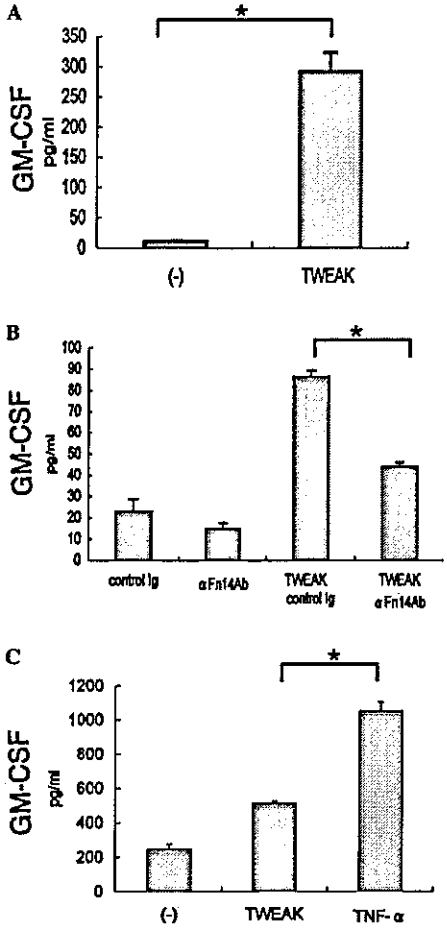

Fig. 3. TWEAK induces GM-CSF production by BEAS2B cells via Fn14. BEAS2B cells were stimulated with 100 ng/ml TWEAK for 48 h (A) or stimulated with 20 ng/ml TWEAK for 24 h in the presence of 10 μg/ml anti-Fn14 blocking mAb or control Ig (B) or stimulated with 10 ng/ml TWEAK or 10 ng/ml TNF-α for 48 h (C). Human GM-CSF concentration in the culture supernatant was measured by ELISA. Data are indicated as means ± SD of triplicate samples. $^*p < 0.05$. Similar results were obtained in three repeated experiments.

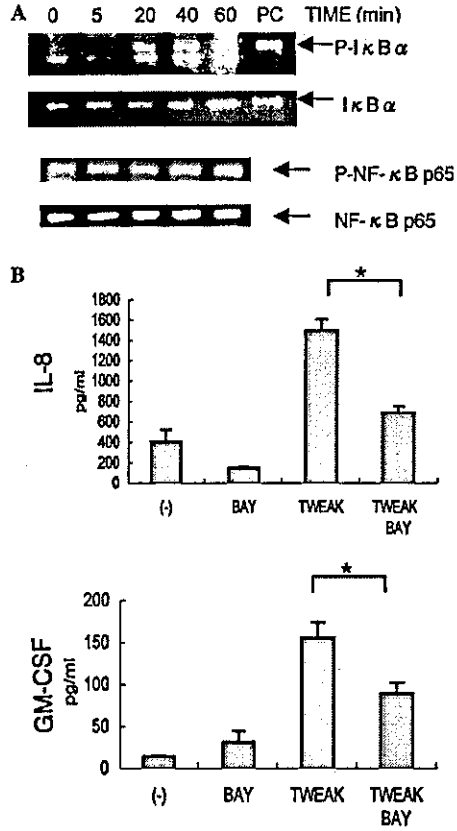

Fig. 4. Critical role of IκBα phosphorylation in TWEAK-induced IL-8 and GM-CSF production by BEAS2B cells. (A) BEAS2B cells were stimulated with 100 ng/ml TWEAK for the indicated time periods. Then, the cell lysates were immunoblotted with anti-phosphorylated IκBα (Ser32) antibody or anti-IκBα antibody or anti-phosphorylated NF-κB p65 antibody (Ser536) or NF-κB p65 antibody. PC: positive control (HeLa cell extract stimulated with TNF-α). Representative of three repeated experiments with similar results. (B) BEAS2B cells were stimulated with 100 ng/ml TWEAK for 24 h in the presence or absence of 2 μM BAY 11-7082. Human IL-8 or GM-CSF concentration in the culture supernatant was measured by ELISA. Data are indicated as means ± SD of triplicate samples. $^*p < 0.05$. Similar results were obtained in three repeated experiments.

IL-8 and GM-CSF and thus may contribute to the development of airway inflammatory responses.

TWEAK induced IL-8 and GM-CSF production by BEAS2B cells and primary cultured bronchial epithelial cells (Figs. 2, 3, and 5). However, MCP-1, TARC, or Eotaxin was not produced by BEAS2B cells upon TWEAK stimulation (data not shown). We and others have previously shown that TWEAK induces several cytokines/chemokines; for example, IL-8 and MCP-1 from human umbilical vein endothelial cells (HUVEC) [6], TNF-α from certain tumor cell lines [16], IL-8, IP-10, and RANTES from human dermal fibroblasts and synoviocytes [7]. Thus, the pattern of cytokines/chemokines induced by TWEAK varies depending on the cell types.

Anti-Fn14 mAb did not completely inhibit GM-CSF production as in Fig. 3B, which was quite different from the inhibition observed in IL-8 production (Fig. 2C). This may suggest the existence of other receptors than Fn14 mediating TWEAK effect leading to GM-CSF production. Polek et al. [17] recently proposed the second receptor for TWEAK that was responsible for osteoclast differentiation. The second receptor for TWEAK may thus exist in human bronchial epithelial cells.

We found that TWEAK induced phosphorylation of IκBα (Fig. 4A). This is consistent with the recent findings by Saitoh et al. [10] that TWEAK stimulated IκBα phosphorylation, resulting in activation of NF-κB in

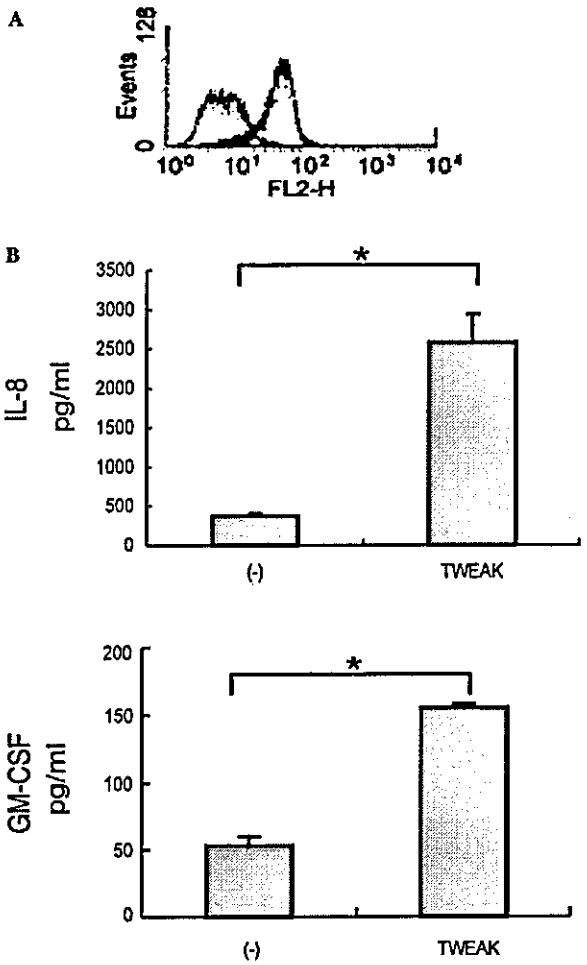

Fig. 5. TWEAK induces IL-8 and GM-CSF production by primary cultured human bronchial epithelial cells. (A) Primary cultured normal human bronchial epithelial cells were stained with biotinylated anti-human Fn14 mAb (right histogram) or control Ig (left histogram), followed by PE-labeled avidin, and then analyzed by flow cytometry. A representative of three repeated experiments with similar results is shown. (B) Primary cultured normal human bronchial epithelial cells were stimulated with 100 ng/ml TWEAK for 48 h. Human IL-8 or GM-CSF concentration in the culture supernatant was measured by ELISA. Data are indicated as means ± SD of triplicate samples. $^*p < 0.05$. Similar results were obtained in three repeated experiments.

fibroblasts. The finding that BAY11-7082, a specific inhibitor of IκBα kinase, abrogated the TWEAK-induced IL-8 and GM-CSF production by BEAS2B cells (Fig. 4B) is also consistent with previous observations that the expressions of IL-8 and GM-CSF genes were NF-κB-dependent [18,19]. However, it should be noted that BAY11-7082 incompletely inhibited IL-8 and GM-CSF production, suggesting the possibility that signaling pathways other than NF-κB might also contribute to TWEAK-induced IL-8 and GM-CSF production by human bronchial epithelial cells.

It remains unclear regarding the role of TWEAK in respiratory disease. Nakayama et al. [4] showed that IFN-γ-stimulated monocytes expressed TWEAK and induced cell death in some tumor cell lines. Thus, we speculate that alveolar or infiltrating monocytes/macrophages might express TWEAK upon inflammation and interaction between the activated monocytes/macrophages and bronchial epithelial cells might play some role in the development of certain inflammatory lung diseases through IL-8 and GM-CSF production. We are currently doing immunohistochemical studies with anti-TWEAK antibodies to identify TWEAK producers in inflammatory lung disorders. We are also examining TWEAK expression in bronchoalveolar lavage fluids obtained from patients with various pulmonary inflammatory disorders.

In summary, we demonstrated a novel biological activity of TWEAK on human bronchial epithelial cells. Our results suggest that TWEAK/Fn14 interaction in bronchial epithelial cells may be involved in the pathogenesis of inflammatory lung diseases.

Acknowledgments

We thank Masufumi Nakayama, Noriko Yamaguchi for discussion and technical assistance, Yuko Ohnuma, and Michiyo Matsumoto for secretarial assistance. This work was supported in part by the grants from the Ministry of Education, Culture, Sports, Science and Technology, Japan and from the Ministry of Health, Labor and Welfare, Japan.

References

[1] Y. Chicheportiche, P.R. Bourdon, H. Xu, Y.M. Hsu, H. Scott, C. Hession, I. Garciha, J.L. Brownin, TWEAK, a new secreted ligand in the tumor necrosis factor family that weakly induces apoptosis, J. Biol. Chem. 272 (1997) 32401–32410.
[2] S.R. Wiley, J.A. Winkles, TWEAK, a member of the TNF superfamily, is a multifunctional cytokine that binds the TweakR/Fn14 receptor, Cytokine Growth Factor Rev. 14 (2003) 241–249.
[3] P. Schneider, R. Schwngzere, E. Haas, F. Muhlenbeck, G. Schubert, P. Scheurich, J. Tschopp, H. Wajant, TWEAK can induce cell death via endogenous TNF and TNF receptor 1, Eur. J. Immunol. 29 (8) (1999) 1785–1792.
[4] M. Nakayama, Y. Kayagaki, N. Yamaguchi, K. Okumura, H. Yagita H, Involvement of TWEAK in interferon-γ-stimulated monocyte cytotoxicity, J. Exp. Med. 192 (2000) 1373–1380.
[5] C.N. Lynch, Y.C. Wang, J.K. Lund, Y.W. Chen, J.A. Leal, S.R. Wiley, TWEAK induces angiogenesis and proliferation of endothelial cells, J. Biol. Chem. 274 (1999) 8455–8459.
[6] N. Harada, M. Nakayama, H. Nakano, Y. Fukuchi, H. Yagita, K. Okumura, Pro-inflammatory effect of TWEAK/Fn14 interaction on human umbilical vein endothelial cells, Biochem. Biophys. Res. Commun. 299 (2002) 488–493.
[7] Y. Chicheportiche, R. Chicheportiche, I. Sizing, J. Thompson, C.B. Benjamin, C. Ambrose, J.M. Dayer, Proinflammatory activity of TWEAK on human dermal fibroblasts and synoviocytes: blocking and enhancing effects of anti-TWEAK monoclonal antibodies, Arthritis Res. 4 (2002) 126–133.

[8] S.R. Wiley, L. Cassiano, T. Lofton, T. Davis-Smith, J.A. Winkeles, V. Lindner, H. Liu, T.O. Daniel, C.A. Smith, W.C. Fanslow, A novel TNF receptor family member binds TWEAK and is implicated in angiogenesis, Immunity 15 (2001) 837–846.

[9] R.L. Meighan-Mantha, D.K. Hsu, Y. Guo, S.A. Brown, S.L. Feng, K.A. Peiffley, G.F. Alberts, N.G. Copeland, D.J. Gilbert, N.A. Jenkins, C.M. Richards, J.A. Winkles, The mitogen-inducible Fn14 gene encodes a type I transmembrane protein that modulates fibroblast adhesion and migration, J. Biol. Chem. 274 (1999) 33166–33176.

[10] T. Saitoh, M. Nakayama, H. Nakano, H. Yagita, N. Yamamoto, S. Yamaoka, TWEAK induces NF-κB2 p100 processing and long-lasting NF-κB activation, J. Biol. Chem. 278 (2003) 36005–36012.

[11] M. Nakayama, K. Ishidoh, Y. Kojima, N. Harada, E. Kominami, K. Okumura, H. Yagita, Fibroblast growth factor-inducible 14 mediates multiple pathways of TWEAK-induced cell death, J. Immunol. 170 (2003) 341–348.

[12] Y. Ke, R.R. Reddel, B.I. Gerwin, M. Miyashita, M. McMenamin, J.F. Lechner, C.C. Harris, Human bronchial epithelial cells with integrated SV40 virus T antigen genes retain the ability to undergo squamous differentiation, Differentiation 38 (1998) 60–66.

[13] K. Yamane, H. Ihn, Y. Asano, M. Jinnin, K. Tamaki, Antagonistic effects of TNF-α on TGF-β signaling through down-regulation of TGF-β receptor type II in human dermal fibroblasts, J. Immunol. 171 (2003) 3855–3862.

[14] C.L. Scaife, J. Kuang, J.C. Wills, B. Trowbridge, P. Gray, B.M. Manning, E.J. Eichwald, R.A. Daynes, S.K. Kuwada, Nuclear factor κB inhibitors induce adhesion-dependent colon cancer apoptosis: implications for metastasis, Cancer Res. 62 (2002) 6870–6878.

[15] H. Takizawa, Airway epithelial cells as regulators of airway inflammation, Int. J. Mol. Med. 1 (1998) 367–378.

[16] M. Nakayama, K. Ishidoh, N. Kayagaki, Y. Kojima, N. Yamaguchi, H. Nakano, E. Kominami, K. Okumura, H. Yagita, Multiple pathways of TWEAK-induced cell death, J. Immunol. 168 (2002) 734–743.

[17] T.C. Polek, M. Talpaz, B.G. Darnay, T. Spivak-Kroizman, TWEAK mediates signal transduction and differentiation of RAW264.7 cells in the absence of Fn14/TweakR, J. Biol. Chem. 278 (2003) 32317–32323.

[18] C. Kunsch, C.A. Rosen, NF-κB subunit-specific regulation of the interleukin-8 promoter, Mol. Cell. Biol. 13 (1993) 6137–6146.

[19] R. Schreck, P.A. Baeuerl, NF-κB as inducible transcriptional activator of the GM-CSF gene, Mol. Cell. Biol. 10 (1990) 1281–1286.